*Journal of Molecular Structure*, 247 (1991) 135-171
Elsevier Science Publishers B.V., Amsterdam

# IR and UV matrix photochemistry and solvent effects: the isomerization of diazocyclohexadienones (ortho quinone diazides) — detection of molecules with the 1,2,3-benzoxadiazole structure. A UV/Vis and IR absorption and UV photoelectron spectroscopic investigation*

Armin Schweig[1] and Horst Baumgartl

*Fachbereich Physikalische Chemie und Zentrum für Materialwissenschaften der Philipps-Universität, W-3550 Marburg (Germany)*

Reinhard Schulz

*Plastics Division, Electronic Materials, Ciba-Geigy Ltd. CH-4002 Basel (Switzerland)*

(Received 22 March 1990)

## Abstract

6-Diazo-2,4-cyclohexadienone and derivatives with fluoro, chloro, methyl, *tert*-butyl and methoxy substituents have been investigated by UV/Vis absorption, IR absorption and UV photoelectron spectroscopy. Spectral results obtained in the gas phase, in an argon matrix at 10 K and in *n*-hexane solution at room temperature reveal an equilibrium with the respective 1,2,3-benzoxadiazole isomers, thus disproving current textbook opinions. The 1,2,3-benzoxadiazole structure is derived from the agreement of observed and calculated vertical ionization energies, characteristic IR and UV/Vis absorption bands as well as selective IR and UV photochemical transformations. The relative concentration of the respective 1,2,3-benzoxadiazole in equilibrium with the diazoketone isomer strongly depends on the substituents and on solvent effects. The diazoketone structure is stabilized by hydrogen bonding and polar interactions. The most stable 1,2,3-benzoxadiazole in this study, the 5,7-di-*tert*-butyl derivative, is at least 6.3 kJ mol$^{-1}$ more stable than its diazocyclohexadienone valence isomer, whereas 2,3,4,5-tetrafluoro-6-diazo-2,4-cyclohexadienone and 3-methoxy-6-diazo-2,4-cyclohexadienone did not isomerize to a notable extent. Energetic considerations for the stabilization of 1,2,3-oxadiazoles are discussed and compared with experimental and theoretical findings.

## INTRODUCTION

The chemistry of 1,2-diazoketones [1], especially in terms of structure, ther-

---

*Dedicated to the memory of Professor George Wilkinson.

[1] Author to whom correspondence should be addressed.

0022-2860/91/$03.50

mal and photochemical reactions, synthetic utility and technological aspects has retained high attention for about a hundred years [2]. Today, this class of compound represents an important pool of intermediates for the synthesis of a wide range of strained [3] and natural [4] products. Particularly 6-diazo-2,4-cyclohexadienone derivatives (*o*-quinone diazides) [5] are of industrial importance for photo-imaging applications, especially for the fabrication of printing plates [6] and photoresists [7], thus contributing to the fast development of information technology and microelectronics.

When 6-diazo-2,4-cyclohexadienones (1,2-benzoquinone diazides) were synthesized for the first time about a hundred years ago [2,8] by diazotisation of 2-aminophenols, methods for elucidation of the structure of these compounds were very limited. At that time and through the following decades the structures **1** to **4** were discussed [9]. From the absorption properties in the near UV and visible region [10], similar to those of benzoquinones, the position of the carbonyl and diazo bands in the IR spectra [11] and dipole moment measurements [12], it was later concluded that the molecular structure is correctly represented by formula **1**. Early work in this field as well as the present status regarding molecular and electronic structure, physical and chemical properties have been recently summarized in reviews [1,5]. There seemed to be no doubt that the structures **2**, **3** and **4** can be definitively excluded for diazotisation products of 2-aminophenols. Consequently, this view has become fixed as a rule in reviews [1a,5c] and textbooks [13].

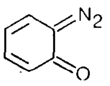

1

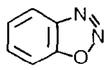

2

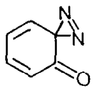

3

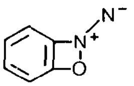

4

As a reason for the apparent instability of **2** and **4** the weakness of the N–O bond (bond enthalpy *E*(A–B) 157 kJ $mol^{-1}$ at 25°C [14]) may be quoted. However, this explanation seems to be insufficient because of the quite high stabilities of 1,2,3-thiadiazoles (**5**), 1,2,3-selenadiazoles (**6**) or 1,2-oxazoles (**7**) and their respective benzo-fused analogs. Furthermore, the 1,2,3-oxadiazole skeleton is stable in the sydnones (**8**) [15], which, however, may be classified as a separate group due to their peculiar mesoionic structure.

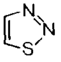

5

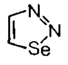

6

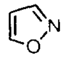

7

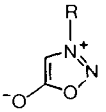

8

Below we present a detailed reinvestigation of the aforementioned problem using the methods of IR and UV matrix photochemistry and absorption spectroscopy, solution absorption spectroscopy as well as UV photoelectron spectroscopy. Based on the photochemical and spectroscopic results obtained, in particular on solvent (hydrogen bonding) effects, an equilibrium between 6-diazo-2,4-cyclohexadienone and various derivatives, and their respective 1,2,3-benzoxadiazole isomers will be revealed, thus disproving current textbook opinions.

## EXPERIMENTAL

### *UV photoelectron spectroscopy*

A sample reservoir, made from borosilicate glass, was connected with the target chamber of a modified Perkin-Elmer PS 16 photoelectron spectrometer via a temperature-controlled inlet system [16]. The inlet system consisted of a 20 cm×0.5 cm stainless-steel tube. The temperature was measured with a chrome–alumel thermocouple and could be varied from room temperature to about 800°C. The temperature of the sample reservoir was controlled by a thermocouple and a regulated electrical heating system. Measurements were performed in the dark to prevent decomposition of the light-sensitive samples. The pressure inside the inlet system was about 5–15 Pa. The spectra were calibrated using acetylene ($^2\Pi_u$ at 11.40 eV) and nitrogen ($^2\Sigma_g^+$ at 15.57 eV and $^2\Pi_u$ at 16.69 eV).

### *Matrix isolation technique and sample preparation*

The apparatus and the procedure were described in preceding [16,17] publications. A sample reservoir for solid compounds was directly attached to the stainless-steel shroud of an Air Products CS 202E Displex cryogenic refrigeration system at the height of the window region and the cold tip. The sample reservoir and the 5 cm×0.4 cm tubing were made from borosilicate and quartz glass and could be gently heated to facilitate evaporation, when necessary. The temperature of the sample reservoir was measured with a thermocouple. The refrigeration system was equipped with a DMX-1A shroud for optical spectroscopy and KBr windows. The temperature of the cold window was controlled by a heater and a 0.07% iron-doped gold vs. chromel thermocouple by using an Air Products APD-B temperature controller. Matrix mixtures were prepared by subliming the sample into a large excess of argon, and matrices were deposited on a KBr window. The temperature of the cold window was maintained at 15 K and the total pressure in the vacuum system at $\approx 5\times10^{-4}$ Pa by additional pumping with a turbomolecular pump.

### *Matrix IR and UV photolysis*

IR irradiation was performed within the sample compartment of the Beckman IR 4250 spectrophotometer by the standard Nernst glower. Additionally, IR filters could be put between sample and radiation source during irradiation or while running spectra. In some experiments a $\lambda > 2.3$ $\mu$m or a $\lambda > 4.5$ $\mu$m long pass filter (Oriel) was used.

UV irradiation was accomplished with a 350 W high pressure mercury lamp (Osram HBO), quartz condenser optics, an 8 cm long water filter with quartz windows (to absorb IR radiation) and narrow band filters (10 nm band pass) or cut-off filters (Schott).

*Matrix and solution UV/Vis absorption spectroscopy*

The UV/Vis absorption spectra were run on a Shimadzu UV-240 or UV-260 spectrophotometer. The spectral resolution was 0.3–0.5 nm. Solvents used for solution spectra were Uvasole quality. Solutions contained $\approx 10^{-4}$ M of the 1,2-benzoquinone diazides (or its 1,2,3-benzoxadiazole isomers). Dissolution speed was generally low in *n*-hexane and stirring or shaking for several minutes was necessary to achieve complete dissolution in this solvent at room temperature.

*Matrix and solution IR absorption spectroscopy*

The IR absorption spectra were recorded on a Beckman IR 4250 spectrophotometer at a resolution of $\approx 1$ cm$^{-1}$ at 1000 cm$^{-1}$.

*Materials*

The 1,2-benzoquinone diazides were synthesized as described below and were stored in the dark in the refrigerator at −18°C. Prior to the experiments they were additionally purified by sublimation in vacuo in the dark or under yellow light (pressure, $\approx 1$ Pa; temperature, 25–55°C).

*6-Diazo-2,4-cyclohexadienone (**1**) [18]*

2-Aminophenol hydrochloride (4.3 g) is diazotized at 0°C with isoamylnitrite (10 ml) in absolute methanol (25 ml). The resulting 2-hydroxyphenyldiazonium chloride is precipitated with cold *tert*-butyl methyl ether, filtered, washed and dried. (Caution! The substance has to be handled like an explosive!) A portion (1 g) of the dry hydroxyphenyldiazonium chloride is added to 2.5 g powdered anhydrous sodium carbonate and the mixture is shaken vigorously until a yellow-brown colour appears (5–10 min). Extraction with 50 ml dry *tert*-butyl methyl ether, filtration and evaporation of the ether in vacuo at room temperature gives 0.6 g of yellow crystals of pure **1**. The preparation should be done under yellow light or in the dark. M.p. of **1**, 65°C (dec.); IR (Ar matrix), 2113(s), 2091(m), 1650(m), 1594(m), 1589(m), 1513(m), 1446(m), 1388(w), 1243(m), 1179(w), 1147(m), 1110(w), 858(w), 835(w), 750(m) and 707(m) $cm^{-1}$; first vertical ionization energy, 8.20 eV ($^2A''(\pi)$).

Based on the IR-induced transformation of **2** to **1**, the IR bands of 1,2,3-benzoxadiazole (**2**) were observed (Ar matrix) at 1615(m), 1605(m), 1485(m), 1465(s), 1440(m), 1437(m), 1365(w), 1342(s), 1295(m), 1261(m), 1222(m), 1119(m), 1005(m), 892(m), 777(m), 763(m), 752(s), 543(m), 493(m), 421(m) and 372(m) $cm^{-1}$. The vertical ionization energies of **2** are 9.45, 9.95 eV (both $^2A''(\pi)$), 11.20 ($^2A'(\sigma_N)$) and 12.37 eV ($^2A''(\pi)$).

On irradiation at $\lambda > 350$ nm 6-fulvenone (**10**) was obtained from **1**, or from **2** on irradiation at $\lambda = 300$ nm (narrow band filter) in an argon matrix or after gas-phase pyrolysis of the gas mixture, containing **1** and **2** at 320 °C. IR bands of **10** (Ar matrix) were at 2138(vs), 2080(m), 1582(w), 1459(m), 1448(m), 1407(m), 1329(m), 1079(m), 899(s), 725(s), 634(m), 573(m) and 518(w) $cm^{-1}$. The vertical ionization energies of **10** are 8.56 eV ($^2A_2(\pi)$) and 9.06 eV ($^2B_1(\pi)$).

*3-Methoxy-6-diazo-2,4-cyclohexadienone (5-methoxy-1,2-benzoquinone-(2)-diazide, **14**) [18d]*

To a solution of 2.76 g 4-methoxy-1,2-benzoquinone in 70 ml dichloromethane, 3.72 g tosylhydrazide in 70 ml dichloromethane are added in small portions at −15 °C. The combined solutions are stored at 0 °C for 1 h in the dark. After concentration to about 40 ml in vacuo, the solution is purified on a column filled with basic alumina, which has been deactivated with methanol. With dichloromethane as an eluent a yellow solution of **14** is obtained. Yield was 53% after evaporation of dichloromethane, m.p. 103 °C after purification by sublimation in vacuo.

IR (Ar matrix) bands were at 2102(s), 1642(s), 1603(s), 1530(w), 1467(w), 1383(w), 1331(s), 1238(w), 1232(m) and 1109(w) $cm^{-1}$. The vertical ionization energies of **14** are 8.00 eV ($^2A''(\pi)$), 9.23 eV ($^2A''(\pi)$ and $^2A'(n_O)$) and 11.02 eV ($^2A''(\pi)$).

Upon irradiation with light of $\lambda > 350$ nm 3-methoxy-6-fulvenone was obtained in argon matrix or on gas-phase pyrolysis at 520 °C, and was characterized by IR bands (in AR matrix) at 2130(s), 1605(s), 1581(m), 1368(m), 1285(w), 1215(w), 1170(w), 1042(w), 911(w) and 752(w) $cm^{-1}$ and vertical ionization energies (gas phase) at 8.02 and 8.84 eV (both $^2A''(\pi)$).

*4-Chloro-6-diazo-2,4-cyclohexadienone (4-chloro-1,2-benzoquinone-(2)-diazide, **16**) [19]*

To a suspension of 1 g of 4-chloro-2-aminophenol in 5 ml of 3 N HCl a saturated solution of 5 g of $NaNO_2$ in water is added with cooling at 0 °C. The product precipitates and the mixture is neutralized with $K_2CO_3$. After filtration, the solid product is dissolved in trichloromethane and purified by chromatography on neutral alumina. After recrystallisation (benzene) and sublimation in vacuo (1 Pa, 80 °C) pure **16** is obtained; yield, 45%, m.p. 99 °C.

IR (Ar matrix) bands were at 2112(s), 2096(s), 1655(m), 1589(m), 1512(m), 1364(m), 1230(m), 1162(m), 1120(w), 921(w), 889(w), 835(w), 820(m), 752(w), 510(m) and 478(w) $\mathrm{cm}^{-1}$. The first vertical ionization energy of **16** was 8.48 eV ($^2A''(\pi)$).

Based on the IR-induced transformation of **19** to **16**, the IR bands of 5-chloro-1,2,3-benzoxadiazole (**19**) were located (Ar matrix) at 1603(m), 1467(s), 1455(s), 1416(m), 1328(m), 1278(m), 1202(s), 1140(w), 823(m), 815(m), 800(m) and 709(m) $\mathrm{cm}^{-1}$. The vertical ionization energies of **19** were 9.42 eV ($^2A''(\pi)$), 10.22 eV ($^2A''(\pi)$), 11.22 eV ($^2A'(\sigma_N)$), 11.90 eV ($^2A'(n_{Cl})$ and $^2A''(\pi)$).

On irradiation with light of $\lambda > 350$ nm 3-chloro-6-fulvenone was obtained from **16**, or from **19** on irradiation at $\lambda = 300$ nm (narrow band filter) in an argon matrix, or after gas-phase pyrolysis of the gas mixture, containing **16** and **19** at 430 °C. IR bands (Ar matrix) were at 2157(s), 2140(s), 1605(m), 1539(m), 1530(m), 1468(s), 1332(s), 1262(m), 1258(m), 1095(m), 1075(m), 1070(s), 918(s), 912(m), 900(m), 786(s), 775(s), 770(m), 662(w), 640(w), 592(w) and 570(m) $\mathrm{cm}^{-1}$ and vertical ionization energies at 8.66 and 9.21 eV (both $^2A''(\pi)$).

### *3,4-Dimethyl-6-diazo-2,4-cyclohexadienone (4,5-dimethyl-1,2-benzoquinone-(2)-diazide, **17**) [18d]*

Compound **17** was synthesized according to a similar procedure to **14**, from 2.72 g 4,5-dimethyl-1,2-benzoquinone and 3.72 g tosylhydrazide. Yield was 61%, m.p. 62–63 °C.

IR (Ar matrix) bands were at 2092(s), 1656(s), 1602(s), 1520(s), 1454(m), 1420(w), 1378(m), 1324(s), 1310(w), 1242(s), 1162(m), 1090(s), 1039(w), 1002(s), 870(m), 858(m), 828(m), 720(w), 712(m) and 680(m) $\mathrm{cm}^{-1}$, and the first vertical ionization energy of **17** is 8.03 eV ($^2A''(\pi)$).

Based on the IR-induced transformation of **20** to **17**, the IR bands of 5,6-dimethyl-1,2,3-benzoxadiazole (**20**) were located (Ar matrix) at 1475(m), 1470(s), 1466(s), 1432(m), 1424(m), 1390(m), 1288(m), 1229(m), 1150(w), 1100(w), 1023(m), 1000(s), 850(s), 838(s) and 568(m) $\mathrm{cm}^{-1}$. Vertical ionization energies of **20** were 9.00 eV ($^2A''(\pi)$), 9.48 eV ($^2A''(\pi)$), 10.86 eV ($^2A'(\sigma_N)$) and 12.00 eV ($^2A''(\pi)$).

Upon irradiation at $\lambda > 350$ nm 3,4-dimethyl-6-fulvenone was obtained from **17** or from **20** on irradiation at 300 nm (narrow band filter) in an argon matrix, or after pyrolysis of the gas mixture, containing **17** and **20** at 450 °C. IR bands (Ar matrix) were at 2130(s), 1520(m), 1517(m), 1490(w), 1458(m), 1449(m), 1420(m), 1350(s), 1295(s), 1025(m), 985(m), 980(m), 925(s), 790(s), 710(w), 648(w), 570(m) and 505(m) $\mathrm{cm}^{-1}$. Vertical ionization energies are 8.20 and 8.50 eV ($^2A_2(\pi)$ and $^2B_1(\pi)$).

### *2,4-Di-*tert*-butyl-6-diazo-2,4-cyclohexadienone (4,6-di-*tert*-butyl-1,2-benzoquinone-(2)-diazide,* **18***) [18d]*

To a solution of 1.4 g 3,5-di-*tert*-butyl-1,2-benzoquinone in 10 ml dichloromethane a solution of 4 g tosylhydrazide in 20 ml dichloromethane is added at 0–5 °C. After 30 min, the product is separated from the reaction mixture by column chromatography on basic alumina, which had been deactivated with methanol (eluent, dichloromethane). After evaporation of the solvent the product is sublimed in vacuo at 60 °C and 1 Pa. Yield was 42%, and m.p. 73 °C.

IR bands were at 2120(s), 1625(m), 1565(s), 1549(s), 1520(m), 1460(m), 1365(m), 1258(m), 1201(m), 1140(m), 904(m), 847(m), 778(m) $cm^{-1}$ in KBr and at 2100(s), 1632(w), 1591(m), 1525(w), 1488(m), 1205(m), 1143(m) and 903(w) $cm^{-1}$ in an Ar matrix. No photoelectron bands of **18** could be observed, since **18** isomerizes in the gas phase almost completely to 5,7-di-*tert*-butyl-1,2,3-benzoxadiazole (**21**).

Based on the IR-induced transformation of **21** to **18**, the IR bands of **21** were located (Ar matrix) at 1491(m), 1470(m), 1451(s), 1445(m), 1400(w), 1390(w), 1368(s), 1275(w), 1256(s), 1210(m), 1188(m), 1005(m), 870(m), 838(m), 772(w), 749(w), 668(m), 527(w) and 473(m) $cm^{-1}$. Vertical ionization energies of **21** are 8.67 and 9.22 eV (both $^2A''(\pi)$).

Upon irradiation at $\lambda > 350$ nm 2,4-di-*tert*-butyl-6-fulvenone was obtained from **18** or from **21** on 300 nm irradiation (narrow band filter) in an argon matrix. IR bands (Ar matrix) were at 2120(s), 1580(w), 1368(s), 1255(s), 1050(m), 830(m) and 753(w) $cm^{-1}$.

### *2,3,4,5-Tetrafluoro-6-diazo-2,4-cyclohexadienone (3,4,5,6-tetrafluoro-1,2-benzoquinone-(2)-diazide,* **25***) [20]*

This compound was prepared by diazotisation (with $NaNO_2$) of 2-aminotetrafluorophenol in 70% sulfuric acid with ice cooling. After extraction with dichloromethane and evaporation of the solvent, the product is sublimed in vacuo at 55 °C and 1 Pa. Yield was 94%.

IR bands (Ar matrix) were at 2120(s), 1700(m), 1651(s), 1642(s), 1603(s), 1590(m), 1552(w), 1471(s), 1412(s), 1303(s), 1179(s), 1125(m), 1060(m), 1020(s), 970(s), 732(m) $cm^{-1}$. Vertical ionization energies of **25** were 8.96 eV ($^2A''(\pi)$), 10.45 eV ($^2A''(\pi)$ and $^2A'(n_0)$) and 11.84 eV ($^2A''(\pi)$).

Upon irradiation at $\lambda > 350$ nm 2,3,4,5-tetrafluoro-6-fulvenone was obtained in an argon matrix or on gas-phase pyrolysis at 390 °C and was characterized by its IR absorption bands (Ar matrix) at 2164(s), 1710(m), 1552(w), 1460(m), 1431(s), 1393(s), 1355(m), 1188(m), 1162(m), 1005(m), 982(m), 971(s), 796(w) and 495(w) $cm^{-1}$ and vertical ionization energies (gas phase) 9.46 eV ($^2A_2(\pi)$) and 9.98 eV ($^2B_1(\pi)$).

TABLE 1

Experimental wavelengths ($\lambda_{max}$(nm)) and logarithm of molar absorption coefficients (log $\epsilon$(M$^{-1}$ cm$^{-1}$) in parentheses) at the band maxima of the solution UV/Vis absorption spectra, experimental wavenumbers ($\tilde{\nu}$(cm$^{-1}$)) at the maxima of the IR absorption spectra as well as vertical ionization energies (*VIE*(eV)) of the various 1,2,3-benzoxadiazoles and 1,2-benzoquinone diazides studied in the present work

| Compound | $\lambda_{max}$ (log $\epsilon$(M$^{-1}$ cm$^{-1}$)) | $\tilde{\nu}$ | *VIE* |
|---|---|---|---|
| **2**[a] | 295(3.3), 244(3.7), 203(4.0)[b] | 1465, 752[c] | 9.45, 9.95, 11.10, 12.37 |
| **19** | 306(3.4), 240(3.7), 208(4.3)[b] | 1467, 1455, 1202, 815, 800, 709[c] | 9.42, 10.22, 11.22, 11.90 |
| **20** | 310(3.3), 230(3.7), 196(4.1)[b] | 1470, 1466, 1229, 850[c] | 9.00, 9.48, 10.86, 12.00 |
| **21** | 301(3.4), 250(3.8), 207(4.3)[b] | 1451, 1445, 1368, 1256, 870, 838[c] | 8.67, 9.22, > 10.5 |
| **1**[a] | 402(3.7), 264(3.8), 214(4.3)[d]<br>395(3.7), 266(3.9)[e] | 2113, 2091, 1650, 1594[c]<br>2175, 2140, 1620[f]<br>2168, 2134[g] | 8.20 |
| **14** | 369(3.6), 286(4.0), 217(4.2)[d]<br>378(3.5), 283(4.1), 217(4.2)[h] | 2102, 1642, 1603[c]<br>2128, 1620[f] | 8.00, 9.23 (two bands), 11.02 |
| **17** | 400(3.6), 270(3.6), 218(4.0)[d] | 2092, 1656, 1602[c]<br>2180, 2135, 1637[k]<br>2170, 2120, 1625[f] | 8.03 |
| **16** | 416(3.7), 250(3.8), 222(4.4)[d] | 2112, 2096, 1655, 1589[c]<br>2120, 1608[f] | 8.48 |
| **18** | 411(3.5), 275(3.7), 211(4.2)[d] | 2100, 1632, 1591[c]<br>2135, 2124, 1625[f]<br>2120, 1622[k] | (not measured)[i] |
| **25** | 396(3.5), 260(3.7), 208(4.0)[d] | 2120, 1651, 1603[c] | 8.96, 1045 (two bands), 11.84 |

[a] For a short communication covering this work and for more detailed spectral data, see refs. 25 and 37.

[b] In $n$-hexane ($\approx 10^{-4}$ M), present work.

[c] In an argon matrix, present work.

[d] In methanol ($\approx 10^{-4}$ M), present work.

[e] In water, see ref. 40.

[f] In KBr, see ref. 18d.

[g] In methanol, see ref. 21.

[h] In $n$-hexane, present work.

[i] Intensity too low.

[k] See ref. 22.

### *Spectral data*

Table 1 summarizes the main spectral data of the 1,2-benzoquinone diazides and 1,2,3-benzoxadiazoles studied in the present work.

## RESULTS AND DISCUSSION

### *1,2,3-Benzoxadiazole*

With the rule of non-existence of 1,2,3-oxadiazoles in mind, we investigated thermal reactions of a series of 1,2-diazoketones, 1,2,3-triazoles and 1,2,3-thia- and selena-diazoles [23] using the technique of variable temperature photoelectron spectroscopy (VTPES) [24]. This study was aimed at the detection and characterization of reactive intermediates formed on thermal decomposition. During this study we noted that 6-diazo-2,4-cyclohexadienone (**1**) gave a gas-phase photoelectron spectrum [25] which was inconsistent with the apparently known and proven molecular structure of **1** [18].

The photoelectron (PE) spectrum contained a small band at 8.20 eV, corresponding to the mass spectrometrically determined appearance potential of 8.26 eV [26] for **1**, and a series of photoelectron bands above 9.45 eV with higher intensity. However, it was surprising that the band series, starting at 9.45 eV, did not match the ionization pattern expected for **1** [25] on the basis of semiempirical calculations and reference compounds. From calculations of the vertical ionization energies of **1** with the semiempirical large scale configuration interaction methods CNDO/S [27a–c] PERTCI [21d,27], MNDO [28] PERTCI and LNDO/S [29] PERTCI as well as by comparison with the photoelectron spectrum of the isoelectronic ketene **9** (first ionization energy of **9**: $^2A''(\pi)$ at 8.43 eV [23a]) we expected the first band of **1** at 8.0–8.5 eV

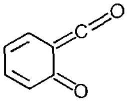

**9**

and further bands above 9.2 eV. According to the calculations, the first photoelectron bands of **1** (up to about 12 eV) should be of similar intensities since the respective ion states could be well represented by one Koopmans configuration each. Thus in agreement with the mass spectrometric measurements [26] the first low intensity band at 8.20 eV was assigned to the first $^2A''(\pi)$ state of **1**. What remained to be explained was the surprising intensity difference between this band and the more intense band sequence above 9.45 eV. Since non-Koopmans effects could be excluded as a reason for the low intensity of the first band, we assigned the bands at 9.45, 9.95, 11.10 and 12.37 eV to ion states of a second molecular species.

After heating the thermal flow reactor [24] to 320°C, 6-fulvenone (**10**) without any byproducts other than $N_2$ was detected PE spectroscopically.

This spectrum of **10** was identical with those which had been obtained independently by exploring other routes [23,30] and did not contain any bands between 10 and 12 eV. Therefore, the intense bands in the spectrum of **1** could not be caused by a decomposition product but had to be ascribed to a compound which also rearranged to 6-fulvenone (**10**) after $N_2$ elimination. Since we could exclude complexes of **1** with itself (i.e. dimers) or with water (H-bond complexes) under the experimental conditions applied[a], the isomers **2**, **3** and **4** had to be considered again.

It is known that in some cases diazirines can be formed photochemically by near UV or visible irradiation from 2-diazoketones [31]. However, it is very unlikely that **3** could be generated by the radiation of the He discharge of the photoelectron spectrometer since photoreactions have never been observed under such conditions. Moreover irradiation of **1** leads to $N_2$ loss and formation of **10** (Scheme 1, see also below) [32]. Furthermore **3** could be excluded due to the lack of a corresponding IR carbonyl band in the low temperature matrix spectra (see below). In addition MNDO calculations yield the following standard enthalpies of formation $\Delta_f H^\ominus(T_c)$ (kJ mol$^{-1}$) 205 (**1**), 159 (**2**), 452 (**3**) and 519 (**4**). Thus **4** is even less stable than **3**, and **3** and **4** are too high in energy to participate in a thermal equilibrium with **1** at room temperature. On the other hand, 1,2,3-benzoxadiazole (**2**) could well account for the remaining bands in the photoelectron spectrum of **1**, the more so since **2** is calculated to be even more stable than **1** by 46 kJ mol$^{-1}$. When this value is corrected by 42 kJ mol$^{-1}$ due to the known underestimation [33] of the nitrogen lone pair repulsion energy, we arrive at a small energetic preference of **2** over **1** of 4 kJ mol$^{-1}$ or at least very similar energies of **1** and **2**. Finally the proposed gas-phase equilibrium $\mathbf{1} \rightleftarrows \mathbf{2}$ is also supported by the good correspondence of observed and calculated vertical ionization energies (VIEs) of **2** [25] as well as the agreement of the first ionization energy of **2** (at 9.45 eV) with an estimated value of 9.5 eV [26].

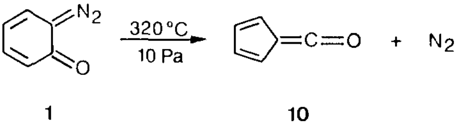

Scheme 1.

Assuming similar ionization cross-sections for the first ionization processes of **1** and **2**, a gas mixture composition of about 10–20% of **1** and 80–90% of **2**

---

[a] Molecular associates, e.g. dimers of carboxylic acids or donor–acceptor complexes can be studied only using special techniques (e.g. expansion through a nozzle from the high pressure side into a vacuum). In a low pressure (5–15 Pa) flow system, as used in the present set-up, such associates are unstable and could not be observed.

could be derived from the relative band intensities. Accordingly, the standard Gibbs function of reaction **1**→**2** $\Delta_r G^{\ominus}(T_c)$ (kJ mol$^{-1}$) amounts to $-4 \pm 1$ which can be taken to be equal to the standard reaction enthalpy $\Delta_r H^{\ominus}(T_c)$ and standard reaction energy $\Delta_r U^{\ominus}(T_c)$ if the standard reaction entropy $\Delta_r S^{\ominus}(T_c)$ is taken to be zero.

The low energy difference of **1** and **2** might be overcome by stabilizing **1** through polar interactions and hydrogen bonding in the solid state and in solution [34]. The presence of the carbonyl group in **1** and a dipole moment of 4.4 D [35] would allow such types of stabilization. In this case one would expect to observe a strong dependence of the UV/Vis absorption spectra of **1**⇄**2** on the polarity and hydrogen-bonding properties of the solvent and isobestic points should occur for spectra recorded as a function of solvent polarity.

The solvent effect on the UV/Vis absorption spectra of some diazoketones has been interpreted in terms of cis–trans isomerization and hydrogen-bonding effects [36]. However, as far as we know there has been no study for 6-diazo-2,4-cyclohexadienones (1,2-benzoquinone diazides) except for our previous communication on **1** [37]. As benzoquinone diazides cannot undergo cis–trans isomerization we have to focus on the possibilities of hydrogen bonding and protonation besides solvent-dependent equilibria as in the case **1**⇄**2**.

In general, 1,2-benzoquinone diazides are yellow or orange coloured compounds and, like their benzo-fused derivatives **11** and **12** [10], have a strong (molar absorption coefficient $\epsilon$ at the band maximum of $\approx 5 \times 10^3$ M$^{-1}$ cm$^{-1}$) UV/Vis absorption band around 400 nm. It follows from the high intensity, that this transition is of the singlet $\pi \to \pi^*$ type, which is corroborated by semiempirical quantum chemical calculations [38]. We have calculated the transition to the first excited $^1A'(\pi\pi^*)$ state of **1** at 378 nm with an oscillator strength of 0.43 using the CNDO/S SECI [39] method and an MNDO-optimized geometry. In full agreement with this result, other authors [38] report that, for **11** and **12**, the first $^1(\pi\pi^*)$ absorption band is calculated at 372 nm using similar procedures. These results contradict previous assignments of the intense 400 nm band to a $\sigma\pi^*$ or a $n\pi^*$ transition [5b]. Such a transition might be assigned, however, to a low intensity shoulder at 500 nm ($\log \epsilon = 1$–$2$ M$^{-1}$ cm$^{-1}$) [10] in the spectra of **11** and **12** and could be hidden under the strong 400 nm band of 1,2-benzoquinone diazides.

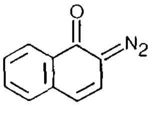

11

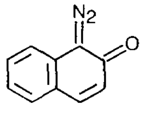

12

On protonation of 1,2-benzoquinone diazides, 2-hydroxybenzene diazonium salts are formed [40]. In aqueous solution these diazonium salts are in equilibrium with the corresponding benzoquinone diazides and the dissociated acid

$H^+X^-$ respectively as shown by conductivity measurements [8e] and UV/Vis absorption spectroscopy [40]. The UV/Vis absorption spectrum of 2-hydroxybenzene diazonium sulfate in water exhibits bands at 395 nm ($\log \epsilon = 3.7\ M^{-1}\ cm^{-1}$) and 266 nm ($\log \epsilon = 3.85\ M^{-1}\ cm^{-1}$), which are characteristic for **1**. After addition of sulfuric acid in excess, the UV/Vis absorption bands of the diazonium compound **13** appear at 353 nm ($\log \epsilon = 3.63\ M^{-1}\ cm^{-1}$) and 266 nm ($\log \epsilon = 4.1\ M^{-1}\ cm^{-1}$). The equilibrium constant for this protonation depends on substituents and a $pK_a$ value of 1.14 was found for the reaction $\mathbf{13} \rightleftarrows H^+ + \mathbf{1}$ [41] (Scheme 2). This means that **1** cannot be protonated to a measurable extent by weak acids or alcohols like methanol ($pK_a = 16$ [42]).

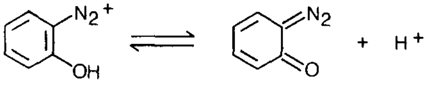

Scheme 2.

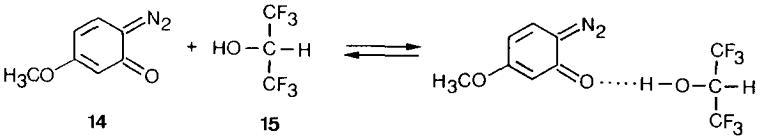

Scheme 3.

To study the effect of hydrogen bonding on UV/Vis absorption spectra we chose 3-methoxy-6-diazo-2,4-cyclohexadienone (**14**) (Scheme 3) as a model compound. This was done for two reasons. Firstly, the presence of the methoxy group in **14** should increase the basicity, facilitating H-bonding and setting an upper limit for less basic derivatives. Secondly, as described later, there was no indication for an equilibrium with the corresponding 1,2,3-benzoxadiazole isomer, which could complicate the spectral interpretation. As an H-donor we used methanol and 1,1,1,3,3,3-hexafluoro-2-propanol (HFIP, **15**, Scheme 3), which is known to be very effective in H-bonding while having only low tendency for self association [43]. Additionally HFIP is transparent in the wavelength region of interest.

Figure 1 shows the UV/Vis absorption spectra of a solution of **14** in *n*-hexane at a concentration of $1 \times 10^{-4}$ M containing different concentrations of HFIP (0–0.2 M). A spectroscopically uniform associate between **14** and HFIP is indicated by an isobestic point at 286 nm. With increasing HFIP concentration the long-wavelength band is continuously shifted from 378 nm (in *n*-hexane) to 364 nm (*n*-hexane containing 0.2 M HFIP). This shift is accompanied by a slight increase in intensity (by a factor of $\approx 1.3$). The second band is influenced to the largest extent, its position shifts from 283 to 298 nm with a similar intensity increase. Additionally a shoulder appears at 235 nm. From a

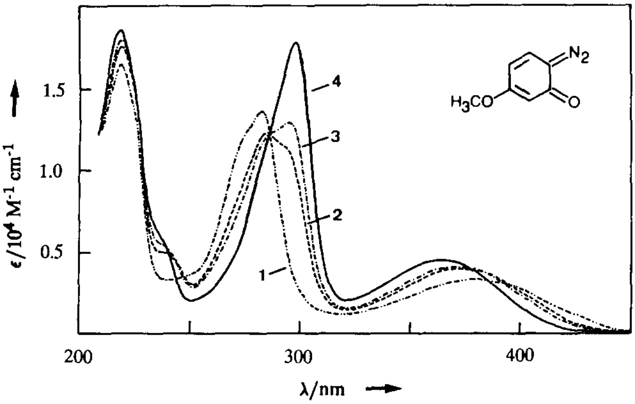

Fig. 1. UV/Vis absorption spectra of 3-methoxy-6-diazo-2,4-cyclohexadienone (**14**) in *n*-hexane and in mixtures of *n*-hexane with 1,1,1,3,3,3-hexafluoro-2-propanol (HFIP, **15**) (molar absorption coefficient, $\epsilon$, vs. wavelength, $\lambda$). HFIP concentrations: 0 (1), 0.005 (2), 0.02 (3) and 0.2 (4) M; $\epsilon$ is referred to the gross (total) concentration of **14** ($10^{-4}$ M).

quantitative evaluation based on the increase of the molar absorption coefficient at 298 nm vs. HFIP concentration a 1:1 complex can be derived[a] for the associate. The spectrum of **14** in methanolic solution ($10^{-4}$ M) is very similar to that of Fig. 1 at a HFIP concentration of 0.005 M (see Fig. 2). Based on these results one could believe that H-bonding will generally induce a blue shift of the 400 nm band of 1,2-benzoquinone diazides of $\approx$ 10–15 nm and a red shift of the second band up to 15 nm, accompanied by only a slight increase in band intensities.

For the parent 6-diazo-2,4-cyclohexadienone (**1**), however, the direction and magnitude of the spectral shifts as well as the changes in intensity are totally different from those observed for **14** when changing from non-polar to polar solvents [37]. As shown in Fig. 2, in *n*-hexane solution only a low intensity band at 408 nm is observed; main absorption maxima are at 295 nm ($\log \epsilon = 3.3$ $M^{-1} cm^{-1}$), 244 nm ($\log \epsilon = 3.7$ $M^{-1} cm^{-1}$) and 203 nm ($\log \epsilon = 4.0$ $M^{-1} cm^{-1}$). When HFIP (**15**) is added, the intensity of the 400 nm band is enhanced by a factor of six (at a HFIP concentration of $2.4 \times 10^{-2}$ M), the 295 nm band disappears in favor of a new band at 264 nm and the band originally at 203 nm is shifted to 214 nm and intensified. The same spectrum (marked 5 in Fig. 2) is obtained, when **1** is dissolved in methanol or water. We note, that only the spectrum obtained in polar, protic solvents (water, methanol or *n*-hexane after

---

[a] For the method used, see ref. 44. The molar absorption coefficient of non-associated **14** (in *n*-hexane) is $\epsilon_B = 3 \times 10^3$ $M^{-1}$ $cm^{-1}$ at 298 nm (i.e. at $\lambda_{max}$ of the associate with HFIP). For high HFIP concentrations the molar absorption coefficient of the associate is determined to be $\epsilon_{ass} \approx 1.85 \times 10^4$ $M^{-1}$ $cm^{-1}$. By plotting $\log [(\epsilon_B - \epsilon'_g)/(\epsilon'_g - \epsilon_{ass})]$ where $\epsilon'_g$ is the measured absorbance at 298 nm divided by the gross concentration of **14** and the thickness of sample vs. the logarithm of the molar concentration of HFIP, a straight line of slope 1 was obtained.

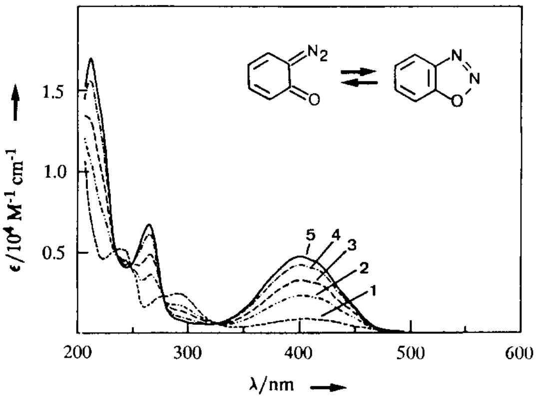

Fig. 2. UV/Vis absorption spectra of 6-diazo-2,4-cyclohexadienone (**1**) in *n*-hexane and in mixtures of *n*-hexane with 1,1,1,3,3,3-hexafluoro-2-propanol (HFIP, **15**) (molar absorption coefficient, ε, vs. wavelength, λ). HFIP concentrations: 0 (1), $2.4\times10^{-3}$ (2), $4.8\times10^{-3}$ (3), $1.2\times10^{-2}$ (4) and $2.4\times10^{-2}$ (5) M; ε is referred to the gross (total) concentration of **1** ($10^{-4}$ M).

addition of HFIP) is explicable in terms of structure **1**, whereas the spectrum obtained in *n*-hexane must be due to a second species in equilibrium with **1** as deduced from the occurrence of isobestic points at 325, 278 and 249 nm. Since H-bonding cannot cause the spectral changes in this case and protonation can be excluded, we suggested a solvent-dependent equilibrium between **1** and **2** (Scheme 4). As estimated from the intensity of the 400 nm band, **2** dominates in *n*-hexane (84% **2** and 16% **1** at a total concentration of $1\times10^{-4}$ M), whereas in methanol almost exclusively **1** is present. CNDO/S SECI calculations of the electronic transition energies of **1** and **2** are in full accord with this conclusion, since they predict for **1** singlet $\pi\rightarrow\pi^*$ transitions at 378 nm (see above), two transitions around 265 nm and one at 227 nm, while for **2** singlet $\pi\rightarrow\pi^*$ transitions are evaluated at around 280 nm, 238 nm and two at ≈205 nm. Furthermore the spectrum ascribed to **2** is similar to that of 1,2,3-benzothiadiazole [37].

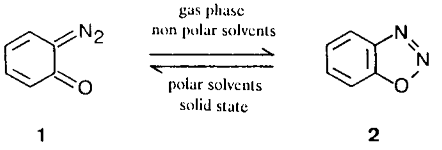

Scheme 4.

The UV/Vis absorption spectroscopic results communicated above clearly corroborate the findings derived from the gas-phase photoelectron spectroscopic investigations and can be further supported by IR spectroscopic results.

When vacuum vaporized **1** is co-condensed with argon at 15 K on a KBr plate, both components of the gas-phase equilibrium **1**$\rightleftarrows$**2** are frozen out and isolated in the solid argon matrix, in which polar interactions are minimized.

We have shown [37], that after co-condensation intense IR absorptions appear, which have to be ascribed to a new compound. During registration of the spectrum with a dispersive IR spectrophotometer this new compound rearranges to **1**, as indicated by the intensity changes of the respective IR bands and by an intensification of the matrix color from light to dark yellow. The IR-induced isomerization follows first-order kinetics with $\tau_{1/2} = 6.2$ min under the conditions applied. Annealing the matrix to 30 K did not change the relative band intensities. By placing a $\lambda > 4500$ nm ($< 2220$ cm$^{-1}$) long pass filter before the Nernst glower, the IR-photoisomerization could be suppressed. This was the only way to record the spectra in the 2200–350 cm$^{-1}$ range without reducing the band intensities of the new compound. However a $\lambda > 2300$ nm ($< 4350$ cm$^{-1}$) long pass filter could not suppress the photoisomerization. The IR absorptions assigned to the new compound on the basis of their intensity changes indicate a 1,2-disubstituted aromatic structure (see Experimental). Particularly the diazirine **3** can be definitively excluded because of the lack of a carbonyl absorption. As mentioned before **4** can be excluded because of its high standard enthalpy of formation.

By irradiation with light of $\lambda > 350$ nm selective cleavage of **1** into $N_2$ and 6-fulvenone (**10**) could be achieved without changing the IR band intensities of the isomeric new compound. This reaction was accompanied by a decoloration of the yellow matrix. Subsequent irradiation at 300 nm through a narrow band filter transformed the new colorless compound to **10** too, which could be easily identified by its known IR absorption bands [45].

From these data we concluded that an equilibrium must exist between **1** and **2** (Scheme 5). In an argon matrix **1** is characterized by its diazo IR band at 2113 cm$^{-1}$ and its carbonyl IR band at 1650 cm$^{-1}$ as well as its dark yellow color which corresponds to the near UV/Vis absorption at 400 nm.

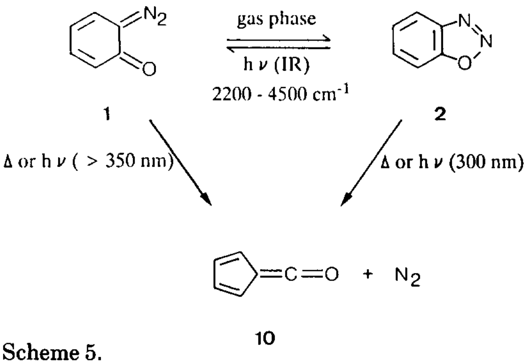

Scheme 5.

Compound **2** is characterized in an argon matrix by IR bands at 1615 and

1605 $cm^{-1}$ (others at 1485, 1440, 1437, 1365, 1342, 1295, 1261, 1222, 1119, 1005, 892, 777, 763, 543, 493, 421 and 372 $cm^{-1}$ with medium intensity) and two stronger ones at 1465 and 752 $cm^{-1}$ and its longest wavelength electronic transition below 350 nm (at about 300 nm).

IR irradiation in the 2200–4500 $cm^{-1}$ spectral range caused ring cleavage of **2** and reformation of **1**. The photon energy corresponding to this spectral range is $40 \pm 14$ kJ $mol^{-1}$. This is an exceptionally low value for a reaction which proceeds with bond cleavage.

Recently an IR-induced intersystem crossing (ISC) of singlet 4-oxo-2,5-cyclohexadienylidene to the more stable triplet state has been reported [46], which might suggest that, in our case, the corresponding 2-oxo-3,5-cyclohexadienylidene could be involved as the species responsible for the observed IR-induced spectral changes. However, the reaction conditions would require that **1** is cleaved into $N_2$ and the resulting carbene in the gas phase at room temperature and that both are trapped in the argon matrix. This can be ruled out because no nitrogen is detected by photoelectron spectroscopy, which would be necessary for the reformation of **1** from such an oxo-carbene in an IR-activated process. Furthermore one would expect that, in a thermal process, the singlet ketocarbene is formed in the first step. However, according to recently performed calculations [47] no minimum could be found for *singlet* 2-oxo-3,5-cyclohexadienylidene on the potential energy hypersurface. Instead the ketocarbene structure collapsed into the 6-fulvenone structure without any further intermediate (e.g. oxirene). Thus nitrogen loss and ring contraction take place in one step. These theoretical results are in full accord with the experimental (thermal and photochemical) findings of the present work.

### *5-Chloro-1,2,3-benzoxadiazole, 5,6-dimethyl-1,2,3-benzoxadiazole and 5,7-di-*tert*-butyl-1,2,3-benzoxadiazole*

Figures 3, 4 and 5 show the gas-phase photoelectron spectra obtained after vaporization of the diazoquinones **16**, **17** and **18** (Scheme 6) at about 5–15 Pa. The similarity between the photoelectron spectrum of vaporized **1** and the photoelectron spectra shown in Figs. 3 and 4 is evident. As for **1** the low intensity ionization band 1a in Figs. 3 and 4 is assigned to the first $^2A''$ ($\pi$) ionization of the respective diazoquinone. This band at 8.48 eV for **16** and 8.03 eV for **17** is only slightly shifted, compared with the 8.20 eV ionization of **1**, due to the chlorine and alkyl substituents.

All the other higher intensity bands are assigned to the corresponding 1,2,3-benzoxadiazole isomers **19** and **20**. The PE band pattern of bands 1, 2 and 3 seems to be characteristic of the 1,2,3-benzoxadiazoles. In the case of **19** a slightly increased splitting of the bands 1 and 2 is observed.

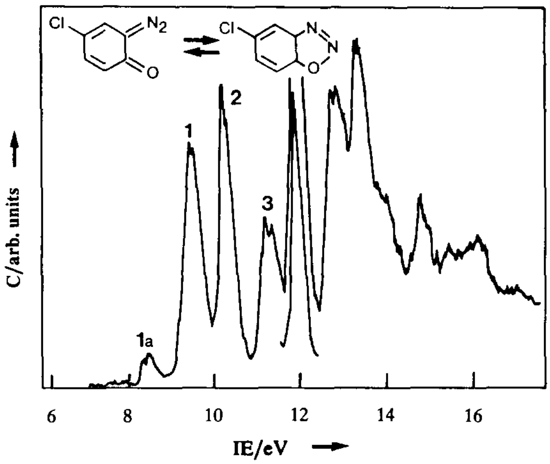

Fig. 3. HeI photoelectron spectrum of vaporized 4-chloro-6-diazo-2,4-cyclohexadienone (**16**, band 1a) in equilibrium with 5-chloro-1,2,3-benzoxadiazole (**19**, bands 1-3 and following bands) (count rate, *C*, vs. ionization energy, *IE*).

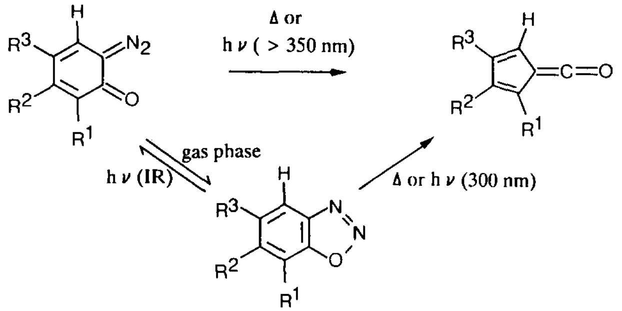

| | **16** | **17** | **18** | **19** | **20** | **21** | **22** | **23** | **24** |
|---|---|---|---|---|---|---|---|---|---|
| $R^1$ | H | H | $C(CH_3)_3$ | H | H | $C(CH_3)_3$ | H | H | $C(CH_3)_3$ |
| $R^2$ | H | $CH_3$ | H | H | $CH_3$ | H | H | $CH_3$ | H |
| $R^3$ | Cl | $CH_3$ | $C(CH_3)_3$ | Cl | $CH_3$ | $C(CH_3)_3$ | Cl | $CH_3$ | $C(CH_3)_3$ |

Scheme 6.

After raising the temperature of the thermal reactor of the photoelectron spectrometer to 440°C, clear-cut PE spectra of the pyrolysis products $N_2$, 3-chloro-6-fulvenone (**22**) and 3,4-dimethyl-6-fulvenone (**23**), respectively were obtained. Isolation of the reactive systems is not possible, however. An unambiguous identification comes from the very characteristic PE spectra of these compounds when the spectra are compared with that of **10**. All 6-fulvenone derivatives give an ionization pattern with an isolated double band system

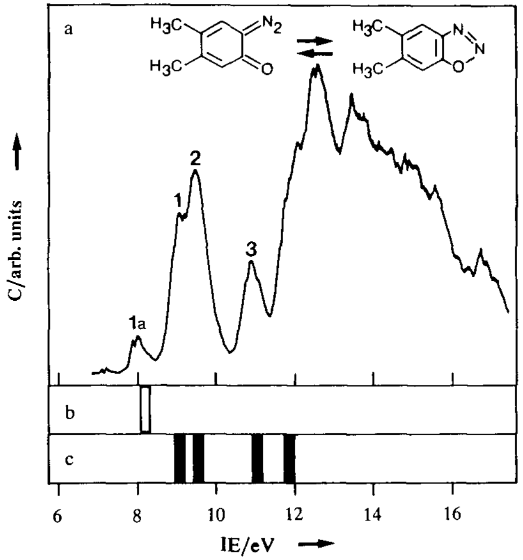

Fig. 4. (a) HeI photoelectron spectrum of vaporized 3,4-dimethyl-6-diazo-2,4-cyclohexadienone (**17**, band 1a) in equilibrium with 5,6-dimethyl-1,2,3-benzoxadiazole (**20**, bands 1-3 and following bands) (count rate, *C*, vs. ionization energy, *IE*). (b) and (c) CNDO/S PERTCI vertical ionization energies (*VIE*) of **17** and **20**, respectively.

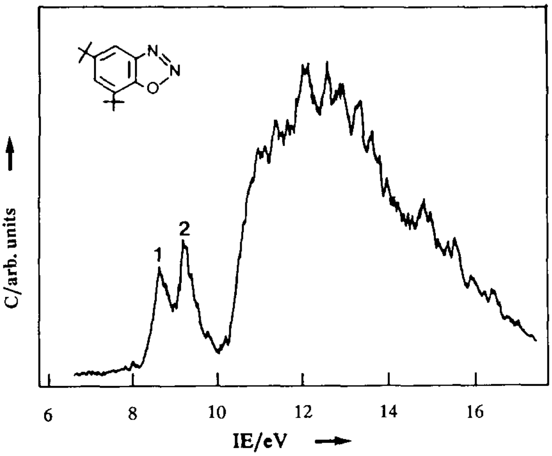

Fig. 5. HeI photoelectron spectrum of 5,7-di-*tert*-butyl-1,2,3-benzoxadiazole (**21**) obtained by evaporation of 2,4-di-*tert*-butyl-6-diazo-2,4-cyclohexadienone (**18**) at a pressure of 5 Pa (count rate, *C*, vs. ionization energy, *IE*).

at the ionization onset, with a gap of about 0.5 eV between the two $\pi$ bands. In **22** only a very small shift of 0.1–0.2 eV towards higher ionization energies relative to parent **10** is observed for the first two bands. In addition, the lone pair ionization bands of the chlorine atom in **22** appear at 11.3–11.7 eV. Because of the alkyl group effect, the PE bands of **23** are shifted to lower ionization energies by about 0.4–0.5 eV. As for **10** neither **22** nor **23** have PE bands in the 10–11 eV range, thus **16**, **17**, **19** and **20** are completely thermolyzed to the corresponding fulvenones and nitrogen (Scheme 5).

Surprisingly, the PE spectrum of vaporized **18** does not exhibit any PE features which could be assigned to ionization processes of a molecule with an *ortho*-quinone like structure (Fig. 5). The first $^2A''$ ($\pi$) ionization of **18** should occur below 8.0 eV if one takes a slightly larger substituent effect of the *tert*-butyl groups vs. the methyl groups in **17** into account. However, no band is observed in this ionization region; instead two bands appear at 8.67 eV and 9.22 eV where one would expect the first ionization processes of the benzoxadiazole **21**.

According to MNDO calculations the first PE band of **21** is expected to occur 1.2 eV higher in energy than the first band of **18**, i.e. at 8.5–9.2 eV. Further support for the presence of **21** instead of **18** in the gas phase can be derived from the substituent effect of the two *tert*-butyl groups which is expected to lower the first $\pi$ ionization energies of aromatic systems (for example benzene [48]) by $\approx$0.8 eV. Thus based on this value and the measured vertical ionization energies of parent 1,2,3-benzoxadiazole (**2**) (9.45 and 9.95 eV [25]) we arrive at 8.65 eV and 9.15 eV for **21**, in excellent agreement with the measured values (compare bands 1 and 2 in Fig. 5). The onset of the $\sigma$-ionization region at 10.5 eV is typical for molecules containing *tert*-butyl groups and obscures the underlying band pattern of the 1,2,3-benzoxadiazole skeleton.

From the intensities of the first ionization bands it is estimated that the 1,2,3-benzoxadiazoles **19**, **20** and **21** dominate over their isomeric diazoquinones by $\approx$90%, $\approx$80% and >95% respectively. These percentages correspond to $\Delta_r U^{\ominus}(T_c)$ values of the various diazoquinones→1,2,3-benzoxadiazole reactions of $-4$, $-3$ and less than $-6$ kJ mol$^{-1}$ or corresponding "greater stabilities" of the various 1,2,3-benzoxadiazoles relative to their quinone diazide counterparts.

The finding that after vaporization of **18** only **21** could be detected in the gas phase by PE spectroscopy is fully reflected in the UV/Vis absorption spectrum of **18** in *n*-hexane solution (Fig. 6(a)). As expected for a 1,2,3-benzoxadiazole structure, intense electronic bands are observed at 301 nm ($\log\epsilon = 3.4$ M$^{-1}$cm$^{-1}$), 250 nm ($\log\epsilon = 3.8$ M$^{-1}$cm$^{-1}$) and 207 nm ($\log\epsilon = 4.3$ M$^{-1}$cm$^{-1}$). In contrast to the colorless solution in hexane, a bright yellow solution is obtained with methanol as a solvent. The yellow color corresponds to the typical diazoquinone singlet $\pi \rightarrow \pi^*$ transition which gives rise to a band at 411 nm ($\log \epsilon = 3.5$ M$^{-1}$cm$^{-1}$). Further electronic bands of **18** occur at 275 nm ($\log\epsilon = 3.7$

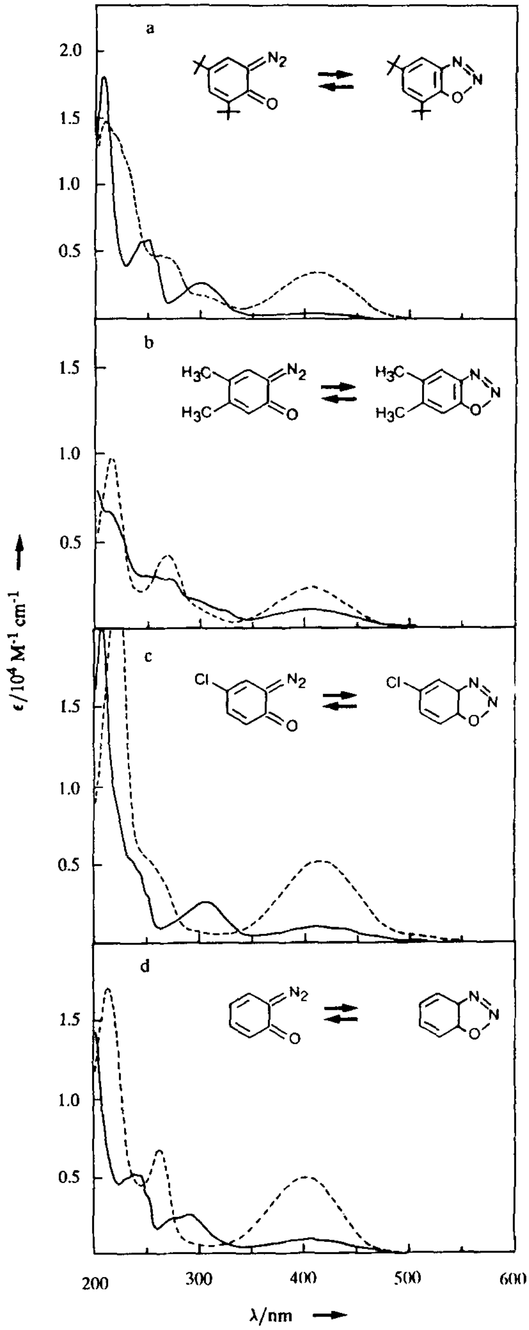

Fig. 6. UV/Vis absorption spectra of (a) 2,4-di-*tert*-butyl-6-diazo-2,4-cyclohexadienone (**18**), (b) 3,4-dimethyl-6-diazo-2,4-cyclohexadienone (**17**), (c) 4-chloro-6-diazo-2,4-cyclohexadienone (**16**) and (d) 6-diazo-2,4-cyclohexadienone (**1**) in *n*-hexane (bold curves) and methanol (dashed curves) at a gross concentration of the solute of $10^{-4}$ M in each case (molar absorption coefficient, $\epsilon$, vs. wavelength, $\lambda$).

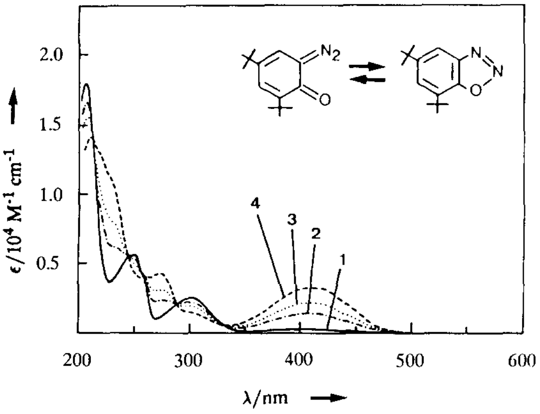

Fig. 7. UV/Vis absorption spectra of 2,4-di-*tert*-butyl-6-diazo-2,4-cyclohexadienone (**18**) in *n*-hexane and mixtures of *n*-hexane with 1,1,1,3,3,3-hexafluoro-2-propanol (HFIP, **15**) (molar absorption coefficient, $\epsilon$, vs. wavelength, $\lambda$). HFIP concentrations: 0 (1), $1.2\times10^{-2}$ (2), $2.4\times10^{-2}$ (3) and $4.8\times10^{-2}$ (4) M; $\epsilon$ is referred to the gross concentration of **18** of $10^{-4}$ M.

$M^{-1}\,cm^{-1}$) and 211 nm ($\log\epsilon=4.2\ M^{-1}\,cm^{-1}$) (see Fig. 6(a)). When HFIP (**15**) is added to the hexane solution containing **21**, the equilibrium **18**$\rightleftarrows$**21** is shifted towards **18** with increasing HFIP concentration. At a gross concentration of $10^{-4}$ M (i.e. sum of the concentrations of **18** and **21**) a HFIP concentration of 0.05 M leads to the same UV/Vis absorption spectrum as that of **18** in methanolic solution. The occurrence of isobestic points at 330, 287, 258, 245 and 213 nm supports the interpretation of the experimental findings in terms of a solvent-dependent equilibrium (Fig. 7). The relative concentration of **18** in *n*-hexane can be estimated from the relative absorbance at 411 nm (relative to the absorbance of **18** in methanol or after addition of HFIP, see Fig. 6(a) and spectrum 4 in Fig. 7) to about 8% of the gross concentration.

The UV/Vis absorption spectrum of the dimethyl derivative **17** in methanol (Fig. 6(b)) displays bands very similar to those of **18** (Fig. 6(a)) and **1** (see Fig. 6(d)). The $^1(\pi\pi^*)$ bands of **17** are at 400 nm ($\log\epsilon=3.6\ M^{-1}\,cm^{-1}$), 270 nm ($\log\epsilon=3.6\ M^{-1}\,cm^{-1}$) and 218 nm ($\log\epsilon=4.0\ M^{-1}\,cm^{-1}$). With *n*-hexane as a solvent a more complex spectrum is obtained which can be explained by the presence of **17** and **20** in the solution in about equal amounts (compare the spectra 2 and 3 in Fig. 7). By subtracting the spectrum of the methanolic solution from the spectrum of the hexane solution the following absorption maxima and $\log\epsilon$ ($M^{-1}\,cm^{-1}$) values can be derived for **20**: 310 nm ($\log\epsilon=3.3\ M^{-1}\,cm^{-1}$), 230 nm ($\log\epsilon=3.7\ M^{-1}\,cm^{-1}$) and 196 nm ($\log\epsilon=4.1\ M^{-1}\,cm^{-1}$).

The UV/Vis absorption spectrum of the chloro derivative **16** in methanol is consistent with the diazoquinone structure and shows bands at 416 nm ($\log\epsilon=3.7\ M^{-1}\,cm^{-1}$), 250 nm ($\log\epsilon=3.8\ M^{-1}\,cm^{-1}$) and 222 nm ($\log\epsilon=4.4\ M^{-1}\,cm^{-1}$) (see Fig. 6(c)). The band which appears in the *n*-hexane solution

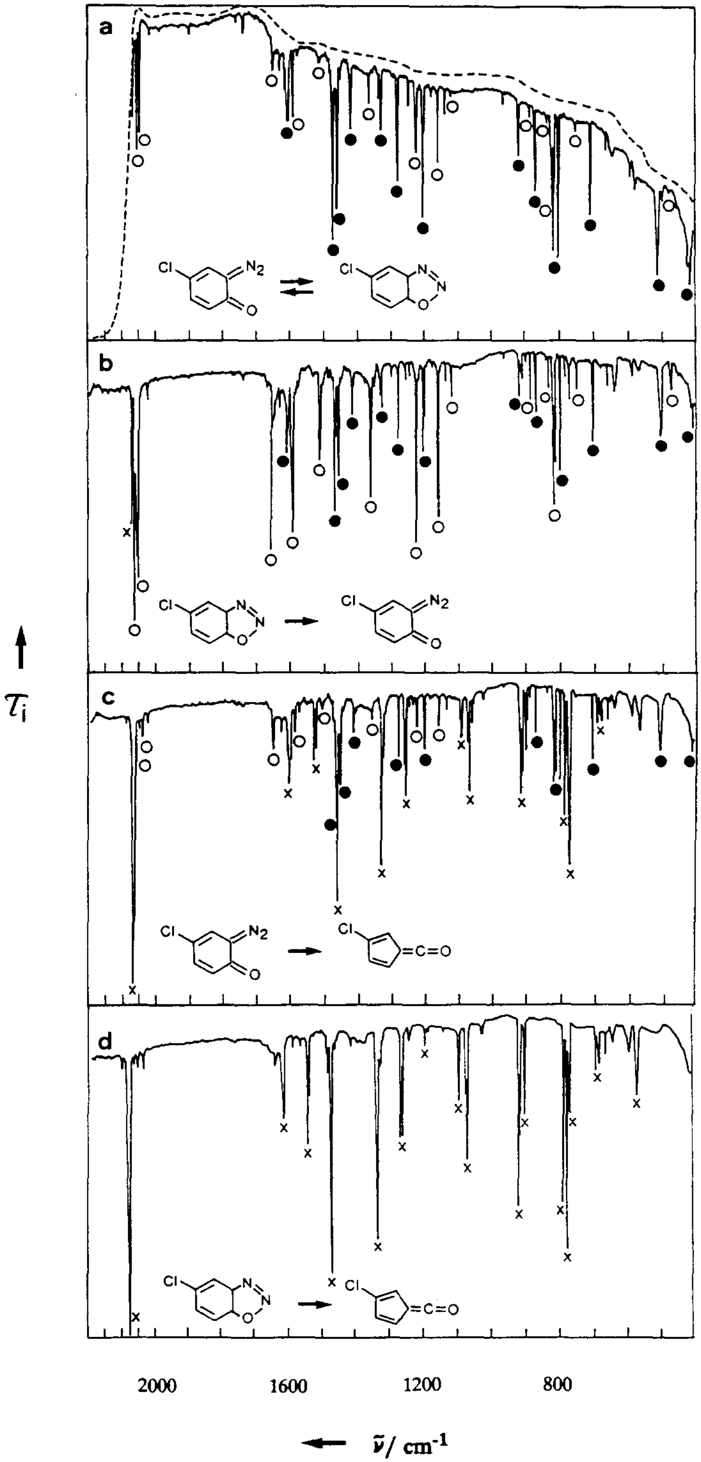
a
Cl
N2
O
b
c
C=O
d
$\mathcal{T}_i$
2000
1600
1200
800
$\tilde{\nu}$/ cm$^{-1}$

at 306 nm ($\log \epsilon = 3.4\ M^{-1}\ cm^{-1}$) is assigned to the longest wavelength singlet $\pi \rightarrow \pi^*$ transition of the oxadiazole **19**.

From the intensity of the 416 nm band in hexane the presence of 15–20% of **16** can be deduced.

In Fig. 6(d) the spectra of **1** in *n*-hexane and methanol are given for comparison. It is obvious that the UV/Vis solution spectra are strictly consistent with the PE spectroscopic gas-phase results and thus strongly back the conclusion reached above regarding the relative stabilities of the 1,2,3-benzoxadiazoles.

Additional evidence for the existence of **19**, **20** and **21** is due to matrix isolation IR absorption spectroscopy. When the diazoquinones **16**, **17** and **18** were vaporized in a vacuum and co-condensed with argon in excess at 20 K, the 1,2,3-benzoxadiazoles **19**, **20** and **21** could be detected by IR spectroscopy as the main components. This is most clearly seen from the IR spectrum of matrix-isolated **18** (Fig. 9 below) where the diazo band is near the detection limit. This result is in full accordance with the PE and UV/Vis spectroscopic findings. Typically, a rather intense IR band is found near 1450 $cm^{-1}$ for the 1,2,3-benzoxadiazoles. This band can be used to monitor their conversion into the corresponding diazoquinones during IR irradiation (2200–4500 $cm^{-1}$, see above). In each case the IR-induced reisomerization is indicated by a yellow discoloration of the matrix and an intensification of the characteristic diazoquinone IR bands (e.g. at about 2100 $cm^{-1}$).

As in the case of **2**, a long pass IR filter was used for blocking the photochemically active IR radiation during recording the spectra of **19**, **20** and **21**. The IR-induced conversion **21**$\rightarrow$**18** was a rather slow process compared to the reactions **2**$\rightarrow$**1**, **20**$\rightarrow$**17**, or **19**$\rightarrow$**16** under identical conditions. Therefore irradiation was performed without any filter behind the Nernst glower in order to gain intensity.

The low photospeed for the IR-driven conversion **21**$\rightarrow$**18** may be due to stronger intramolecular energy dissipation caused by additional degrees of

---

Fig. 8. (a) IR absorption spectrum of an Ar matrix-isolated mixture of 4-chloro-6-diazo-2,4-cyclohexadienone (**16**) and 5-chloro-1,2,3-benzoxadiazole (**19**) obtained after evaporating **16** and co-condensing the gas with argon at 15 K (internal transmittance, $\tau_i$, vs. wavenumber, $\tilde{\nu}$; range of $\tau_i$ from 0 to 1). Bands due to **16** and **19** are marked ○ and ●, respectively. The internal transmittance of the long wave pass filter, $\lambda > 4.5\ \mu m$, used is indicated as a dotted line. (b) IR absorption spectrum of the matrix-isolated photoproducts obtained upon irradiation of the mixture of **16** and **19** described above (part a) with a Nernst glower through a long wave pass filter, $\lambda > 2.4\ \mu m$. As a result bands due to **19** are decreased in intensity whereas bands arising from **16** are intensified. (c) IR absorption spectrum of the products from the aforementioned photoproducts (see part b above) obtained after irradiation with photons of $\lambda > 350$ nm. As a result **16** is selectively converted to 3-chloro-6-fulvenone (**22**) (bands marked ×); band intensities of **19** remain unchanged. (d) IR absorption spectrum of 3-chloro-6-fulvenone (**22**) which is obtained as the sole product from the UV photoproducts (irradiation at $\lambda > 350$ nm, see part c above) upon irradiation at $\lambda = 300$ nm.

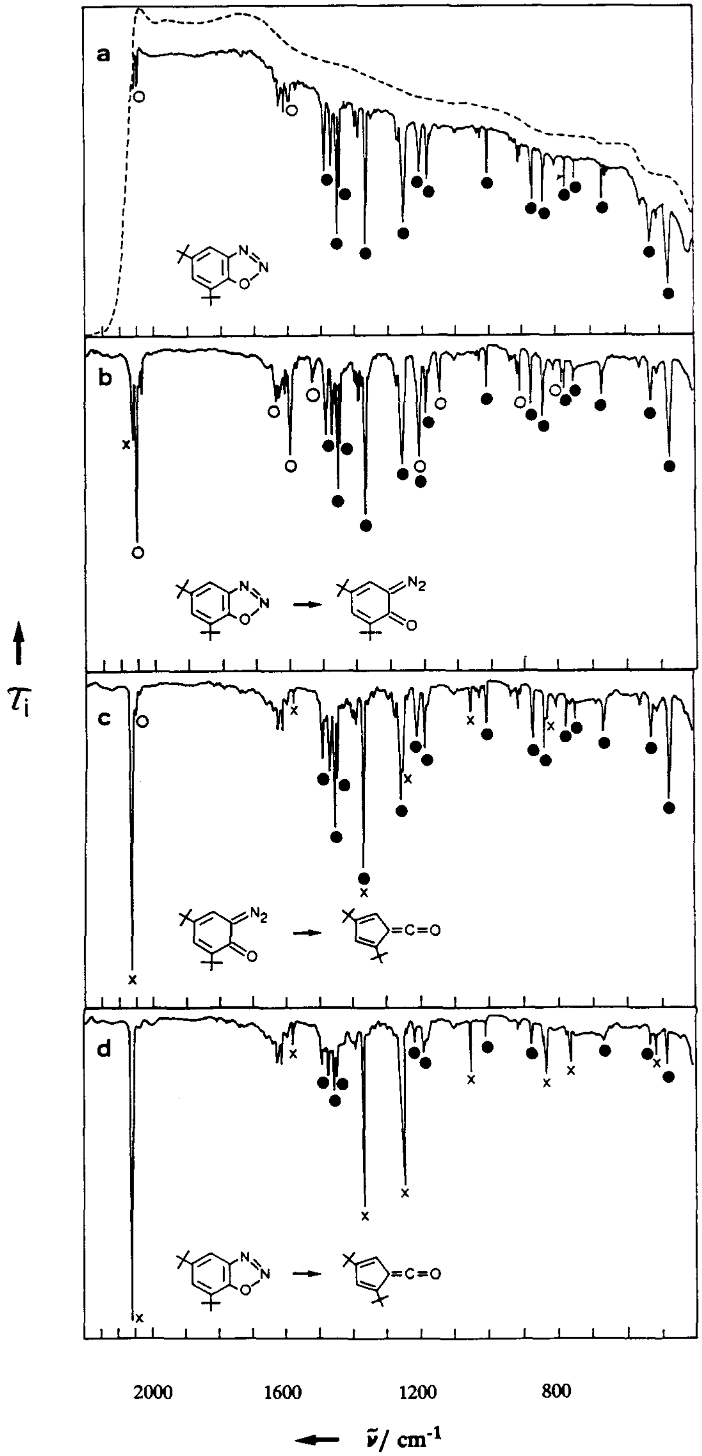
a
b
c
d
N
N
O
N2
O
=C=O
x
$\tau_i$
2000
1600
1200
800
$\tilde{\nu}$/ cm$^{-1}$

freedom which are introduced by the large *tert*-butyl groups or more simply to a higher energy barrier for this reaction compared to the others. In the latter case the *tert*-butyl groups would stabilize the 1,2,3-benzoxadiazole to a greater extent than the transition state of the reaction **21**→**18**.

By irradiation at wavelengths $>350$ nm the diazoquinones **16**, **17** and **18** could be selectively converted to the corresponding colorless 6-fulvenones **22**, **23** and **24** (see for example Figs. 8 and 9). Finally the remaining 1,2,3-benzoxadiazoles **19**, **20** and **21** could be photochemically converted to these 6-fulvenones by irradiation at a wavelength of 300 nm, which corresponds to the longest wavelength singlet $\pi \rightarrow \pi^*$ transition of the benzoxadiazoles. Thus the same behavior was observed as for **1** and **2** (see above).

In an argon matrix the C=C=O vibrational band of the 6-fulvenones (**22**–**24**) was sufficiently separated from the diazoketone C=N=N vibrational band so that both types of compounds could be distinguished.

Figures 8 and 9 give examples for the matrix IR spectra recorded for the co-condensed gas mixtures and the spectral changes observed during subsequent IR and UV photochemical reactions. Band positions observed for the individual compounds are summarized in the experimental section.

### *3-Methoxy-6-diazo-2,4-cyclohexadienone and 2,3,4,5-tetrafluoro-6-diazo-2,4-cyclohexadienone*

Within the class of 6-diazo-2,4-cyclohexadienones studied so far[a] the 3-methoxy compound (**14**) and the 2,3,4,5-tetrafluoro compound **25** showed

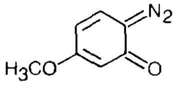

**14**

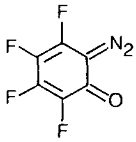

**25**

Fig. 9. (a) IR absorption spectrum of an Ar matrix-isolated mixture of 2,4-di-*tert*-butyl-6-diazo-2,4-cyclohexadienone (**18**) and 5,7-di-*tert*-butyl-1,2,3-benzoxadiazole (**21**) obtained after evaporating **18** and co-condensing the gas with excess argon at 15 K (internal transmittance, $\tau_i$, vs. wavenumber, $\tilde{\nu}$). Bands due to **18** and **21** are marked o and ●, respectively. $\tau_i$ of the long wave pass filter, $\lambda > 4.5$ μm, used is shown as a dotted line. (b) IR absorption spectrum of matrix a (see above) after irradiation with the unfiltered radiation from the Nernst glower of the IR spectrophotometer. Note the appearance of the bands of **18**. (c) IR absorption spectrum of matrix b (see above) upon irradiation with light of $\lambda > 350$ nm. Selective conversion of **18** to 2,4-di-*tert*-butyl-6-fulvenone (**24**, bands marked × in the spectrum) is observed. (d) IR absorption spectrum of matrix c after irradiating matrix c at 300 nm.

---

[a] We have not considered $NO_2$-substituted benzoquinone diazides in the present study because of their explosive nature (especially when heated) and because $NO_2$ groups complicate the UV/Vis absorption spectra in that they give rise to an additional band at $\approx 320$ nm.

no tendency to isomerize to a 1,2,3-benzoxadiazole in the gas phase, solution (*n*-hexane or methanol) or an argon matrix.

Therefore these compounds can serve as reference compounds for the evaluation of the spectral properties of *o*-quinone diazides under the applied conditions, i.e. to support the assignments of the photoelectron spectra, UV/Vis and IR absorption spectra above.

The photoelectron spectrum of **14**, as shown in Fig. 10, displays ionization bands at 8.00, 9.23 (two ionizations) and at 11.02 eV in full accord with the results of CNDO/S PERTCI calculations, which predict ionizations 2 and 3 to be very close in energy. For the isomeric 6-methoxy-1,2,3-benzoxadiazole, however, two band groups consisting of two narrowly spaced bands each and separated by ≈ 2 eV, with the first band group centered at ≈ 9 eV, are predicted by the calculations. From the band intensities of the spectrum in Fig. 10 there is no doubt that we are dealing with a single component spectrum (band 1 similar in intensity to band 4 and of half the total intensity of bands 2 and 3) that must be ascribed to **14**.

A very similar PE spectrum is obtained for **25**, with the bands being shifted by ≈ 1 eV to higher energies, because of the electron-attracting fluoro substituents. Again, the same arguments as for **14** apply and support the diazoketone structure of **25** in harmony with CNDO/S PERTCI calculations (Fig. 11). The solvent effect on the UV/Vis absorption spectrum of **14** has already been discussed above. The UV/Vis absorption spectra shown in Fig. 12(a) are in accord with the effects expected from the study of HFIP as an H donor and

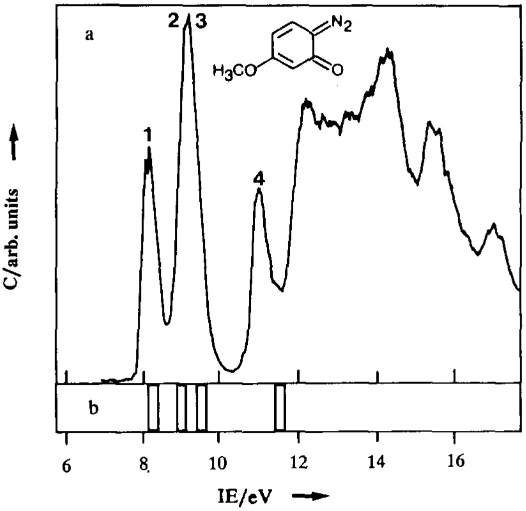

Fig. 10. (a) HeI photoelectron spectrum of vaporized 3-methoxy-6-diazo-2,4-cyclohexadienone (**14**) (count rate, *C*, vs. ionization energy, *IE*). (b) CNDO/S PERTCI vertical ionization energies of **14**.

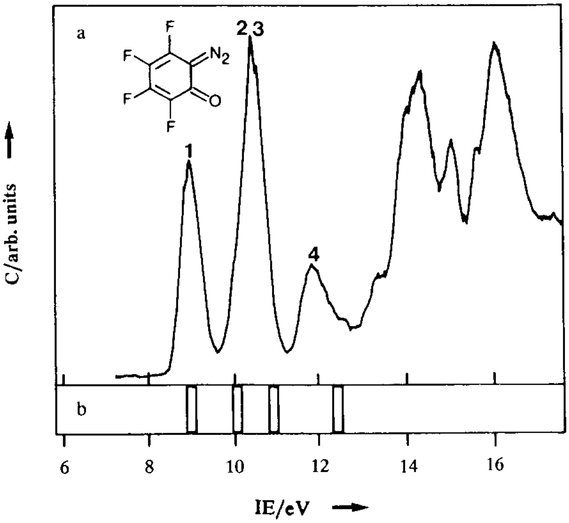

Fig. 11. (a) HeI photoelectron spectrum of 2,3,4,5-tetrafluoro-6-diazo-2,4-cyclohexadienone (**25**) (count rate, *C*, vs. ionization energy, *IE*). (b) CNDO/S PERTCI vertical ionization energies of **25**.

only slight changes in band positions and intensities are observed when using methanol instead of *n*-hexane as the solvent. Figure 12(b) shows the UV/Vis absorption spectra of **25** in *n*-hexane and methanol. Compound **25** is even less susceptible to H-bonding, because the fluorine atoms reduce the electron density at the oxygen atom. This may be the reason for the weak solvent effect in this case. Band positions and molar absorption coefficients for **14** and **25** can be considered to be typical for 1,2-benzoquinone diazides.

We also isolated **14** and **25** in argon at 15 K and subjected the matrices to IR and UV irradiation. The IR spectra of **14** and **25** had strong bands around 2100, 1650 and 1600 cm$^{-1}$, characteristic of quinone diazides, and they did not change on IR irradiation. Irradiation with $\lambda > 350$ nm light converted the dark yellow matrix completely into a colorless one by formation of 3-methoxy-6-fulvenone or tetrafluoro-6-fulvenone respectively. Subsequent irradiation at 300 nm did not produce any further changes.

In summary, we conclude that **14** and **25** are more stable than their 1,2,3-benzoxadiazole isomers by at least 8 kJ mol$^{-1}$ and that polar interactions and hydrogen bonding can reverse the relative stabilities in cases where the 1,2,3-benzoxadiazole is more stable than the corresponding diazoquinone by $\approx 8$ kJ mol$^{-1}$ or less as shown in previous examples. (Note that the limit of 8 kJ mol$^{-1}$ is simply derived by assuming a relative detection limit of the minor component of 3% and that the equilibrium is reached at 20°C.)

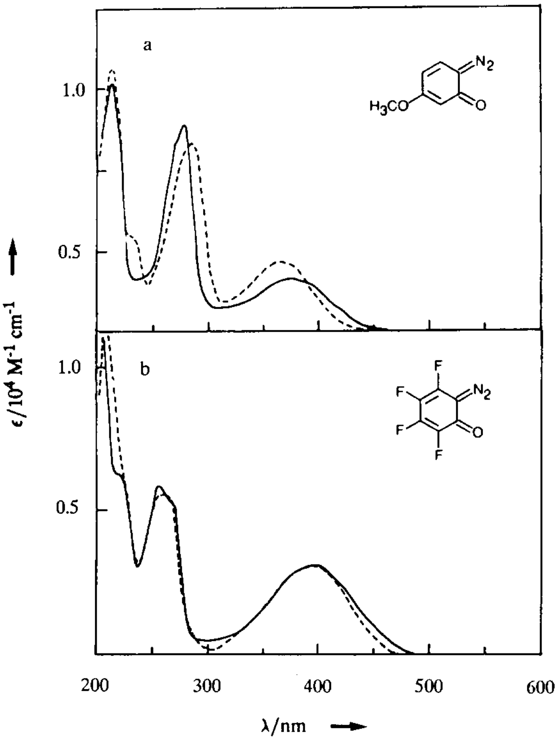

Fig. 12. (a) UV/Vis absorption spectra of 3-methoxy-6-diazo-2,4-cyclohexadienone (**14**) in *n*-hexane (bold curve) and methanol (dashed curve) (molar absorption coefficient, $\epsilon$, vs. wavelength, $\lambda$). (b) UV/Vis absorption spectra of 2,3,4,5-tetrafluoro-6-diazo-2,4-cyclohexadienone (**25**) in *n*-hexane (bold curve) and methanol (dashed curve).

## *Further studies*

Evidence for the existence of 1,2,3-benzoxadiazoles is also provided by room temperature IR spectra of dilute solutions of 6-diazo-2,4-cyclohexadienones. For example, the IR spectrum of a solution of **18** in $CCl_4$ (15 mg in 0.3 ml) contains only weak absorption bands specific of the diazoquinone structure at 2100, 1625, 1580, 1204, 1140, and 905 $cm^{-1}$ in contrast to the high intensity of these bands when recorded in $CHCl_3$ solution at the same concentration or as a KBr pellet. In $CCl_4$ an additional strong band appears at 1448 $cm^{-1}$ which we ascribe to **21** (1451 $cm^{-1}$ in an Ar matrix, see above).

No indications for equilibria with 1,2,3-oxadiazoles could be found for compounds with structures of the types **11**, **12** and **26–29**. Compound **30** is unknown; in the light of the present results it should be unstable with respect to its isomerization to **31**.

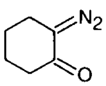

26

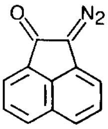

27

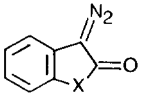

X = O, S

28

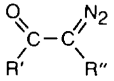

R',R'' = H, alkyl, O-alkyl

29

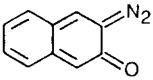

30

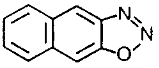

31

Furthermore, the UV/Vis absorption spectra of **32**–**34** in *n*-hexane clearly indicated the predominant presence of the diazoquinone structures since the intense absorption band at 400 nm hardly changed after addition of HFIP or when recorded in methanolic solution.

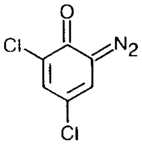

32

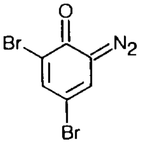

33

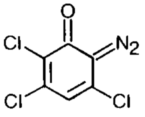

34

### *Relative "stabilities" of 6-diazo-2,4-cyclohexadienones and 1,2,3-benzoxadiazoles*

To predict the prevailing isomer in reactions of the type 1,2-diazoketone→1,2,3-oxadiazole we have performed MNDO calculations of the standard reaction energies $\Delta_r U^\ominus(T_c)$. We found **2** to be 46 kJ mol$^{-1}$ more stable than **1**, whereas the experimental findings point to an energy difference (standard reaction entropy $\Delta_r S^\ominus(T_c)$ assumed to be zero, see above) of only about 4 kJ mol$^{-1}$. Thus a correction of 42 kJ mol$^{-1}$ has to be made to the MNDO results (due to an underestimation of lone pair repulsion). Taking into account this correction, the calculations correctly predict the instability of tetrafluoro-1,2,3-benzoxadiazole (**35**) (21 kJ mol$^{-1}$ less stable than **25**) and of **18** (17 kJ mol$^{-1}$ less stable than **21**) and also of the parent 1,2,3-oxadiazole (**36**) (33 kJ mol$^{-1}$ less stable than formyldiazomethane (**37**)).

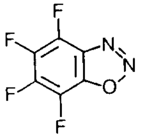

35

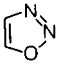

36

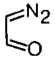

37

Also in accordance with the experimental results, the calculations predict similar energies for **16** and **19** as well as for **17** and **20**. However, similar energies were also computed for **14** and the methoxy-benzoxadiazole **38** which is obviously not correct. The reason for this failure is not yet understood.

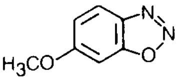

38

Ab initio calculations have been performed [49] on the parent 1,2,3-oxadiazole/formyldiazomethane system. These calculations predict the former to be 37 kJ mol$^{-1}$ higher in energy with an activation barrier of 16 kJ mol$^{-1}$ for the ring cleavage. A comparison with MNDO results reveals, that 1,2,3-oxadiazole can be significantly stabilized by benzanellation (by about 38 kJ mol$^{-1}$ referred to the zero level of energy common to both open systems). Thus, also from these calculations **1** and **2** become very similar in energy.

Since the IR radiation which causes ring cleavage of **2** is in the range 2200–4500 cm$^{-1}$, the activation barrier for this process can be estimated to be $40 \pm 14$ kJ mol$^{-1}$ (the most intense absorption bands within this range are due to the C–H stretching modes at $\approx 3100$ cm$^{-1}$). By combination of the theoretical and experimental data a unified energy diagram for the 1,2,3-oxadiazole/formyldiazomethane and the 1,2,3-benzoxadiazole/6-diazo-2,4-cyclohexadienone systems can be constructed (Fig. 13).

The substituent effect on the relative stability of the 1,2,3-benzoxadiazole/*o*-benzoquinone diazide system cannot be understood on the basis of simple electron attracting or donating properties alone. More detailed studies including variations of position and type of the substituents are necessary to discover the rules which govern this isomerization.

The fact that polar interactions and hydrogen bonding stabilize the (dipolar) 1,2-benzoquinone diazide structure to a greater extent than the less polar 1,2,3-benzoxadiazole structure explains why the former was exclusively found in previous work. The medium effect becomes obvious if the positions of the C=N=N and C=O vibrational bands of 6-diazo-2,4-cyclohexadienones are compared for an argon matrix, a KBr pellet, nujol mull or polar solvents. Frequently the C=N=N band is registered in an argon matrix at a lower wavenumber ($\approx 20$ to 90 cm$^{-1}$ lower) than in the crystalline state or in alcoholic solution, whereas the C=O band is recorded in an argon matrix at higher wavenumbers

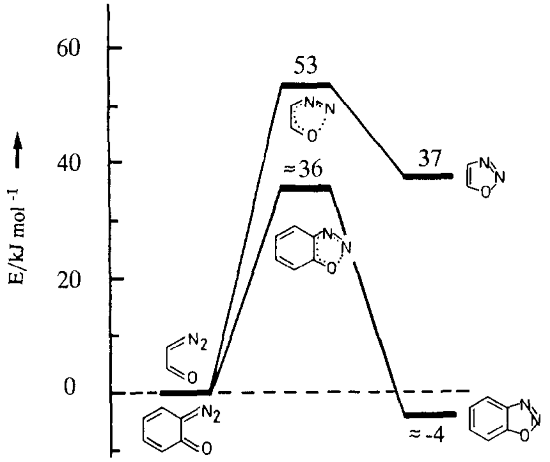

Fig. 13. Approximate energy profiles of the analogous reaction of formyldiazomethane (**37**) $\rightleftarrows$ 1,2,3-oxadiazole (**36**) and 6-diazo-2,4-cyclohexadienone (**1**) $\rightleftarrows$ 1,2,3-benzoxadiazole (**2**). The energies of **37** and **1** are arbitrarily set at zero and the energy values given for **36** and **2** as well as for the barrier heights are relative to the energies of **37** and **1**. For the origin of the various values, consult the text.

($\approx 30\ \mathrm{cm}^{-1}$ higher) than in the solid (KBr pellet or nujol mull). Thus interaction of the carbonyl group with electron acceptors ($\delta^+$) increases the N=N strength (bond order) in favor of a diazonium structure, whereas the C=O bond strength (bond order) decreases in favor of a phenolic structure. Such interaction occur in the solid state and with polar or protic solvents (see **39** and **40** below).

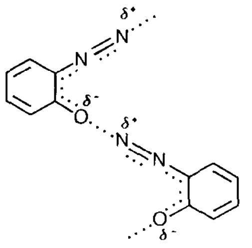

solid state

39

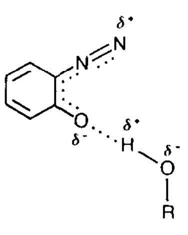

H-bonding

40

## CONCLUSION

1,2,3-Benzoxadiazoles can be detected in the gas phase by UV photoelectron spectroscopy, after condensation in an argon matrix by IR spectroscopy, and in solution (non-polar aprotic solvents) by UV/Vis absorption spectroscopy in equilibrium with their 1,2-benzoquinone diazide (6-diazo-2,4-cyclohexadienone) isomers. The spectroscopic properties are summarized in Table 1. The relative stabilities of 1,2,3-benzoxadiazoles depend strongly on medium effects and substituents.

Ring cleavage of 1,2,3-benzoxadiazoles, isolated in an argon matrix, can be accomplished by IR radiation (2200–4500 $cm^{-1}$), which sets an upper limit for the energy barrier of this reverse isomerization at $40 \pm 14$ kJ $mol^{-1}$.

From the relative intensities of the spectral bands, the energy difference between free unsubstituted 1,2-benzoquinone diazide (**1**) and free 1,2,3-benzoxadiazole (**2**) is estimated to be $4 \pm 1$ kJ $mol^{-1}$ (**1** being more stable than **2**). The most stable 1,2,3-benzoxadiazole derivative found so far is the 5,7-di-*tert*-butyl compound which is at least 6 kJ $mol^{-1}$ more stable than its 1,2-benzoquinone diazide isomer in the gas phase.

1,2,3-Benzoxadiazoles are characterized by a strong IR band at about 1450 $cm^{-1}$ (in an argon matrix) and by a longest wavelength UV/Vis absorption band at around 300 nm. Irradiation or pyrolysis leads to nitrogen loss and formation of the corresponding 6-fulvenone derivatives.

## ACKNOWLEDGMENTS

This work was supported by the Deutsche Forschungsgemeinschaft and the Fonds der Chemischen Industrie. The calculations were carried out on the TR440, Sperry 1100/62, VAX 11/750 and IBM 4381 computers of the Rechenzentrum der Universität Marburg. We thank Dr. Hermann Meyer for critically reading the manuscript.

## REFERENCES

1 (a) S. Patai (Ed.), The Chemistry of Diazonium and Diazo Groups, Wiley, New York, 1978.
(b) M. Regitz and G. Maas, Diazo Compounds, Properties and Synthesis, Academic Press, Orlando, FL, 1986.
2 P. Griess, Justus Liebigs Ann. Chem., 106 (1858) 123.
3 (a) D. Redmore and C.D. Gutschke, Adv. Alicyclic Chem., 3 (1971) 125.
(b) W. Kirmse, Carbene Chemistry, Academic Press, New York, 1971.
(c) D.S. Wulfman and B. Poling, in R.A. Abramovitch (Ed.), Reactive Intermediates, Vol. 1, Plenum Press, New York, London, 1980.
4 T. Hudlicky, D.B. Reddy, S.V. Govindan, T. Kulp, B. Still and J.P. Sheth, J. Org. Chem., 48 (1983) 3422.
5 (a) M.S. Dinaburg, Photosensitive Diazo Compounds, Focal Press, New York, 1964.
(b) V.V. Ershov, G.A. Nikiforov and C.R.H.I. de Jonge, Quinone Diazides, Elsevier, Amsterdam, Oxford, New York, 1981.
(c) P. Grünanger, in Houben-Weyl, Methoden der Organischen Chemie, Vol. 7/3b, Thieme, Stuttgart, 1979.

(d) K.H. Saunders, The Aromatic Diazo Compounds and their Technical Applications, Arnold, London, 1949.

6 O. Süs, J. Munder and H. Stephan, Angew. Chem., 74 (1962) 985.

7 (a) De Forest, Photoresist. McGraw-Hill, New York, 1975.

(b) H. Steppan, G. Buhr and H. Vollmann, Angew. Chem., 94 (1982) 471; Angew. Chem. Int. Ed. Engl., 21 (1982) 455.

(c) I.F. Thompson, C.G. Willson and M.J. Bowden (Eds.), Introduction to Microlithography, ACS Symp. Ser., Vol. 219, American Chemical Society, Washington, 1983.

(d) W.M. Moreau, Semiconductor Lithography, Principles, Practices and Materials, Plenum Press, New York, 1988.

8 (a) P. Griess, Justus Liebigs Ann. Chem., 116 (1860) 123.

(b) H. Silberstein, J. Prakt. Chem., 27 (1883) 98.

(c) E. Bamberger, Ber. Dtsch. Chem. Ges., 28 (1895) 837.

(d) E. Bamberger, Justus Liebigs Ann. Chem., 390 (1912) 154.

(e) A. Hantzsch and W.B. Davidson, Ber. Dtsch. Chem. Ges., 29 (1896) 1522.

(f) R. Meldola, G. Woolcott and E. Wray, J. Chem. Soc., 69 (1896) 1321.

9 Beilstein, Handbuch der Organischen Chemie, Vol. 16, System No. 2197-2207 (1933) and Supplements I (1934), II (1951) and III (1974).

10 L.C. Anderson and M.J. Roedel, J. Am. Chem. Soc., 67 (1945) 955.

11 (a) K.B. Whetsel, G.F. Hawkins and F.E. Johnson, J. Am. Chem. Soc., 78 (1956) 3360.

(b) R.J.W. LeFevre, J.B. Sousa and R.L. Werner, J. Chem. Soc., (1954) 4686.

12 J.D.C. Anderson, R.J.W. LeFevre and R. Wilson, J. Chem. Soc., (1949) 2082.

13 (a) T.L. Gilchrist, Heterocyclic Chemistry, Pitman, London, 1985.

(b) K.T. Potts (Ed.), Comprehensive Heterocyclic Chemistry, Vol. 6, Part 4B, Pergamon Press, Oxford, 1984.

14 P.W. Atkins, Physical Chemistry, Oxford University Press, Oxford, 1986.

15 J.M. Tien and I.M. Hunsberger, J. Am. Chem. Soc., 83 (1961) 178.

16 R. Schulz, A Schweig, K. Hartke and J. Köster, J. Am. Chem. Soc., 105 (1983) 4519.

17 J. Kreile, N. Münzel, A. Schweig and H. Specht, Chem. Phys. Lett., 124 (1986) 140.

18 (a) M. Puza and D. Doetschman, Synthesis, (1971) 481.

(b) B.S. Kikot, J. Gen. Chem. USSR, 33 (1963) 221.

(c) R. Clinging, F.M. Dean and G.H. Mitchell, Tetrahedron, 30 (1974) 4065.

(d) L. Horner and W. Dürckheimer, Chem. Ber., 95 (1962) 1206.

19 R. Huisgen and R. Fleischmann, Justus Liebigs Ann. Chem., 623 (1959) 47.

20 J.M. Birchall, R.N. Haszeldine and E.S. Wilks, J. Chem. Soc., (1971) 562.

21 L.A. Kazitzyna, B.S. Kikot, L.E. Vinogradova and D.A. Reutov, Dokl. Akad. Nauk SSSR, 158 (1964) 1369.

22 W. Ried and R. Dietrich, Chem. Ber., 94 (1961) 387.

23 (a) R. Schulz and A. Schweig, Tetrahedron Lett., (1979) 59.

(b) R. Schulz, Diploma Thesis, Universität Marburg, 1979.

(c) R. Schulz and A. Schweig, Tetrahedron Lett., 21 (1980) 343.

(d) R. Schulz and A. Schweig, Angew. Chem., 92 (1980) 52; Angew. Chem. Int. Ed. Engl., 19 (1980) 69.

(e) R. Schulz and A. Schweig, Tetrahedron Lett., 25 (1984) 2337.

(f) R. Schulz and A. Schweig, Z. Naturforsch., Teil B, 39 (1984) 1536.

24 (a) R. Schulz and A. Schweig, in J. Liebman and A. Greenberg (Eds.), Structure and Reactivity, VCH, New York, 1988.

(b) H. Bock and B. Solouki, Angew. Chem., 93 (1981) 425.

25 R. Schulz and A. Schweig, Angew. Chem., 91 (1979) 737; Angew. Chem. Int. Ed. Engl., 18 (1979) 692.

26 O. Thorstadt and K. Undheim, Chem. Scr., 6 (1974) 222.

27 (a) J. DelBene and H.H. Jaffé, J. Chem. Phys., 48 (1968) 1807, 4050.
(b) R.L. Ellis, G. Kuehnlenz and H.H. Jaffé, Theor. Chim. Acta, 26 (1972) 131.
(c) G. Kuehnlenz and H.H. Jaffé, J. Chem. Phys., 58 (1973) 2238.
(d) H.L. Hase, K.-W. Schulte and A. Schweig, Theor. Chim. Acta, 48 (1978) 47.
28 (a) M.J.S. Dewar and W. Thiel, J. Am. Chem. Soc., 99 (1977) 4899.
29 (a) G. Lauer, K.-W. Schulte and A. Schweig, J. Am. Chem. Soc., 100 (1978) 4925.
(b) W. Zittlau, Doctoral Dissertation, Universität Marburg, 1984.
(c) A. Heidenreich, H. Meyer and A. Schweig, in preparation.
30 H. Bock, T. Hirabayashi and S. Mohmand, Chem. Ber., 114 (1981) 2595.
31 (a) E. Voigt and H. Meier, Chem. Ber., 108 (1975) 3326.
(b) T. Miyashi, T. Nakajo and T. Mukai, J. Chem. Soc., Chem. Commun., (1978) 442.
(c) T. Livinghouse and R.V. Stevens, J. Am. Chem. Soc., 100 (1978) 6479.
(d) E.D. Laganis, D.S. Janik, T.J. Curphy and D.M. Lemal, J. Am. Chem. Soc., 105 (1983) 7457.
32 O. Süs, Justus Liebigs Ann. Chem., 556 (1944) 65, 85.
33 E. Fos, J. Vilarrasa and J. Fernandez, J. Org. Chem., 50 (1985) 4894.
34 (a) C. Reichardt, Solvents and Solvent Effects in Organic Chemistry, VCH, Weinheim, 1988.
(b) P. Beak, Acc. Chem. Res., 10 (1977) 186.
(c) C. Wentrup and H.W. Winter, J. Am. Chem. Soc., 102 (1980) 6159.
35 G. Tappig, Gazz. Chim. Ital., 71 (1941) 111.
36 (a) I.G. Csizmadia, S.A. Houlden, O. Meresz and P. Yates, Tetrahedron, 25 (1969) 2121.
(b) L.L. Leveson and C.W. Thomas, Tetrahedron, 22 (1966) 209.
(c) C. Pecile, A. Föffani and S. Ghersetti, Tetrahedron, 20 (1964) 823.
37 R. Schulz and A. Schweig, Angew. Chem., 96 (1984) 494; Angew. Chem. Int. Ed. Engl., 23 (1984) 509.
38 R.D. Miller, D.R. McKean, T.L. Tompkins, C.G. Willson, J. Michl and J. Downing, in T. Davidson (Ed.), Polymers in Electronics, ACS Symp. Ser., Vol. 242, American Chemical Society, Washington, 1984.
39 (a) K.-W. Schulte and A. Schweig, Theor. Chim. Acta, 33 (1974) 19.
(b) K.-W. Schulte, Doctoral Dissertation, Universität Marburg, 1977.
40 J. DeJonge, R.J.H. Alink and R. Dijkstra, Rec. Trav. Chim. Pays-Bas, 69 (1950) 1448.
41 L.A. Kazitzyna, N.D. Klueva and N.N. Kazanova, Vestnik MGU, Ser. Khim., Moscow State University, (1967) 68.
42 (a) A. Unmack, Z. Phys. Chem., 129 (2927) 439.
(b) A. Unmack, Z. Phys. Chem., 131 (1928) 371.
(c) A. Unmack, Z. Phys. Chem., 133 (1928) 45.
(d) P. Ballinger and F.A. Long, J. Am. Chem. Soc., 82 (1960) 795.
43 J. Juffernbruch and H.-H. Perkampus, Spectrochim. Acta, Part A, 39 (1983) 905, 1093, 1097.
44 H.-H. Perkampus, UV-VIS-Spektroskopie und ihre Anwendungen, Springer, Berlin, 1986.
45 (a) R. Schulz, Doctoral Dissertation, Universität Marburg, 1983.
(b) M. Torres, A. Clement and O.P. Strausz, J. Org. Chem., 45 (1980) 2271.
46 W. Sander, W. Müller and R. Sustmann, Angew. Chem., 100 (1988) 577; Angew. Chem. Int. Ed. Engl., 27 (1988) 572.
47 M. Tsuda and S. Oikawa, J. Photopolym. Sci. Technol., 2 (1989) 235.
48 H. Bock and W. Kaim, Chem. Ber., 111 (1978) 3552.
49 M.T. Nguyen, A.F. Hegarty and J. Elguero, Angew. Chem., 97 (1985) 704; Angew. Chem. Int. Ed. Engl., 24 (1985) 713.

## APPENDIX

**In collaboration with Jens Georg Günther Simon, Harald Specht and Andreas**

Heidenreich (Fachbereich Physikalische Chemie und Zentrum für Materialwissenschaften der Philipps-Universität, Marburg)

The foregoing investigation did not include UV/Vis absorption spectra of matrix-isolated *o*-quinone diazides and 1,2,3-benzoxadiazoles nor did it include LNDO/S PERTCI calculations of the spectra. In conjunction with the solvent effects discussed it would be very desirable, however, to have the pure spectra of at least one *o*-quinone diazide and one 1,2,3-benzoxadiazole in solid argon in order to support the conclusions, drawn from solvent effects, in the foregoing study.

For these reasons we recorded the matrix UV/Vis absorption spectra of the parent 6-diazo-2,4-cyclohexadienone (**1**) (Fig. A1(a)) and 1,2,3-benzoxadiazole (Fig. A2(a)) and compared them with the LNDO/S PERTCI spectra (Figs. A1(b) and A2(b) and Table A1). It is most important to note that the spectra of the open and closed forms in solid argon are very nearly the same as those previously obtained in methanol and *n*-hexane, respectively, with isobestic points occurring at 252, 279 and 308 nm, thus fully supporting the inter-

TABLE A1

Calculated vertical electronic transition wavelengths (nm) and oscillator strengths (in parentheses) along with experimental transition wavelengths at the band maxima for 6-diazo-2,4-cyclohexadienone (**1**) and 1,2,3-benzoxadiazole (**2**) in solid argon

| Molecule[a] | Excited state[a,b] | LNDO/S PERTCI[a,c] | Band[d] | Experimental[e] |
|---|---|---|---|---|
| 6-Diazo-2,4-cyclohexadienone | $\tilde{A}\ ^1A'\ (\pi\pi^*)$ | 354/376 (0.21) | 1 | 406 |
| | $\tilde{B}\ ^1A''\ (\pi\sigma^*)$ | 309/325 (0.006) | | |
| | $\tilde{C}\ ^1A'\ (\pi\pi^*)$ | 258/269 (0.02) | 2 | 265 |
| | $\tilde{D}\ ^1A'\ (\pi\pi^*)$ | 247/257 (0.02) | | |
| | $\tilde{E}\ ^1A'\ (\pi\pi^*)$ | 228/237 (0.20) | 3 | 210 |
| | $\tilde{F}\ ^1A'\ (\pi\pi^*)$ | 214/222 (0.40) | | |
| 1,2,3-Benzoxadiazole | $\tilde{A}\ ^1A'\ (\pi\pi^*)$ | 288/302 (0.04) | 1 | 289 |
| | $\tilde{B}\ ^1A''\ (n\pi^*)$ | 262/273 (0.02) | 2 | 243 |
| | $\tilde{C}\ ^1A'\ (\pi\pi^*)$ | 241/250 (0.05) | | |
| | $\tilde{D}\ ^1A''\ (\pi\sigma^*)$ | 223/231 (0.001) | | |
| | $\tilde{E}\ ^1A'\ (\pi\pi^*)$ | 213/220 (0.23) | 3 | 201 |
| | $\tilde{F}\ ^1A'\ (\pi\pi^*)$ | 200/206 (0.59) | | |

[a] Calculations based on the MNDO optimized ground-state geometry.

[b] Transitions with oscillator strengths of less than 0.001 omitted.

[c] LNDO/S PERTCI wavelengths/LNDO/S PERTCI wavelengths after taking into account the medium effect of solid argon (red shift of ≈0.2 eV).

[d] Numbering of bands as in Figs. A1 and A2.

[e] In an argon matrix from the present work.

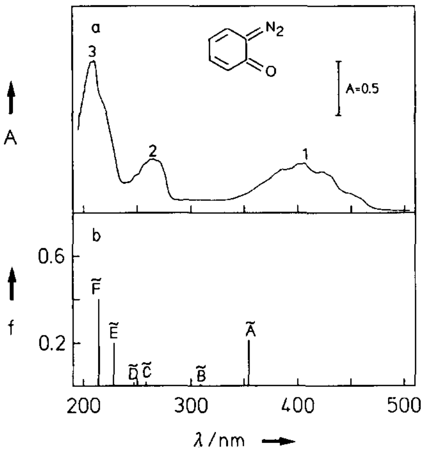

Fig. A1. (a) The UV/Vis absorption spectrum of Ar matrix-isolated 6-diazo-2,4-cyclohexadienone (**1**) (absorbance, *A*, vs. wavelength, *λ*). The bands are numbered in the order of decreasing wavelength. (b) Stick diagram (positions representing the LNDO/S PERTCI vertical electronic transition wavelengths and heights representing the oscillator strengths) for **1**. Note that the LNDO/S PERTCI data shown are not corrected for the medium effect of solid argon. For the notation and assignments of the various states shown, see Table A1 and text.

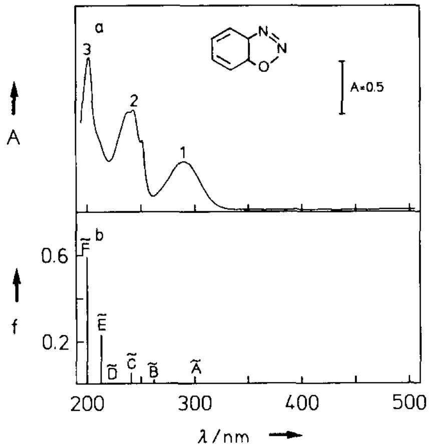

Fig. A2. (a) The UV/Vis absorption spectrum of Ar matrix-isolated 1,2,3-benzoxadiazole (**2**) (absorbance, *A*, vs. wavelength, *λ*). The bands are numbered in the order of decreasing wavelength. (b) Stick diagram (positions representing the LNDO/S PERTCI vertical electronic transition wavelengths and heights representing the oscillator strengths) for **2**. Note that the LNDO/S PERTCI data shown are not corrected for the medium effect of solid argon. For the notation and assignments of the various states shown, see Table A1 and text.

pretation of the solvent dependent spectra in terms of an equilibrium between both forms in the foregoing study.

The comparison between theory and experiment suggests that the bands in both spectra essentially originate from singlet $\pi \rightarrow \pi^*$ transitions except for a singlet $n \rightarrow \pi^*$ transition of medium intensity (oscillator strength $f=0.02$) for **2** and two low intensity ($f=0.006$ and $0.001$) singlet $\pi \rightarrow \sigma^*$ transitions for **1** and **2**, respectively. Note that there is an additional $^1A'$ ($\pi\pi^*$) state calculated below the first one for **1** with an extremely low intensity ($f=0.00002$) which, however, could not be detected in the matrix spectra. Finally, it must be mentioned that the assignments made in Table A1 and Figs. A1 and A2 are ad hoc assignments, only based on the comparison of the experimental spectra with the LNDO/S PERTCI data, and are thus not secured by independent experimental arguments.